Cell Reports

Article

Protective plant immune responses are elicited by bacterial outer membrane vesicles

Graphical Abstract

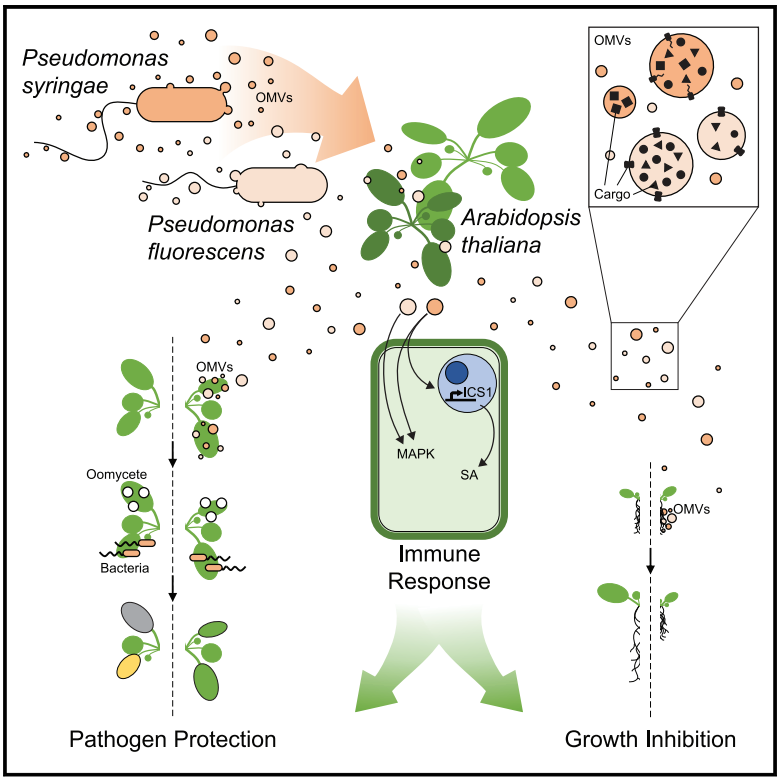

Highlights

- OMVs from *P. syringae* and *P. fluorescens* protect against bacteria and oomycetes
- Bacterial OMVs elicit distinct sets of plant immune responses
- OMV-mediated effects withstand biochemical disruption
- OMVs can serve as new tools to probe the plant immune system

Authors

Hannah M. McMillan, Sophia G. Zebell, Jean B. Ristaino, Xinnian Dong, Meta J. Kuehn

Correspondence

meta.kuehn@duke.edu

In Brief

The role that bacterial outer membrane vesicles (OMVs) play in plant-microbe interactions is poorly characterized. McMillan et al. show that OMVs elicit plant immune responses that protect against pathogens. This study also reveals a use for OMVs as tools to probe the plant immune system.

McMillan et al., 2021, Cell Reports *34*, 108645
January 19, 2021
https://doi.org/10.1016/j.celrep.2020.108645

CellPress

Cell Reports

CellPress
OPEN ACCESS

Article

Protective plant immune responses are elicited by bacterial outer membrane vesicles

Hannah M. McMillan,[1] Sophia G. Zebell,[2] Jean B. Ristaino,[3] Xinnian Dong,[2] and Meta J. Kuehn[1,4,5,*]
[1]Department of Molecular Genetics and Microbiology, Duke University, Durham, NC 27710, USA
[2]Howard Hughes Medical Institute, Department of Biology, Duke University, Durham, NC 27708, USA
[3]Department of Entomology and Plant Pathology, North Carolina State University, Raleigh, NC 27695, USA
[4]Department of Biochemistry, Duke University, Durham, NC 27710, USA
[5]Lead contact
*Correspondence: meta.kuehn@duke.edu
https://doi.org/10.1016/j.celrep.2020.108645

SUMMARY

Bacterial outer membrane vesicles (OMVs) perform a variety of functions in bacterial survival and virulence. In mammalian systems, OMVs activate immune responses and are exploited as vaccines. However, little work has focused on the interactions of OMVs with plant hosts. Here, we report that OMVs from *Pseudomonas syringae* and *P. fluorescens* activate plant immune responses that protect against bacterial and oomycete pathogens. OMV-mediated immunomodulatory activity from these species displayed different sensitivity to biochemical stressors, reflecting differences in OMV content. Importantly, OMV-mediated plant responses are distinct from those triggered by conserved bacterial epitopes or effector molecules alone. Our study shows that OMV-induced protective immune responses are independent of the T3SS and protein, but that OMV-mediated seedling growth inhibition largely depends on proteinaceous components. OMVs provide a unique opportunity to understand the interplay between virulence and host response strategies and add a new dimension to consider in host-microbe interactions.

INTRODUCTION

Cells from all of the kingdoms of life produce extracellular vesicles. Bacteria can use these secreted, 40–200 nm in diameter, biological "packages" to eliminate toxic compounds such as misfolded proteins, facilitate bacterial adaptation to environmental change and stress, and communicate with their environment using insoluble mediators (Orench-Rivera and Kuehn, 2016; Schwechheimer and Kuehn, 2015; McBroom and Kuehn, 2007; Kuehn and Kesty, 2005; Volgers et al., 2018; Florez et al., 2017; Horspool and Schertzer, 2018). In Gram-negative bacteria, vesicles bud from the outer membrane in a process that does not damage or weaken the bacterial membrane (Kulp and Kuehn, 2010; Schwechheimer et al., 2013; McBroom and Kuehn, 2007; Zhou et al., 1998; Beveridge, 1999). Outer membrane vesicle (OMV) production is influenced by many factors, including growth stage and stress, with previous research suggesting that production peaks during late log and early stationary phase and increases in response to stress (Kulp et al., 2015; McBroom and Kuehn, 2007; Schwechheimer et al., 2013; Orench-Rivera and Kuehn, 2016; Schwechheimer and Kuehn, 2015; Berleman and Auer, 2013; Pathirana and Kaparakis-Liaskos, 2016). For bacterial pathogens, studies have shown that OMVs are enriched in toxins and virulence factors and specifically interact with, and are often internalized into, host cells (Schwechheimer and Kuehn, 2015; McBroom and Kuehn, 2007; Kuehn and Kesty, 2005; Volgers et al., 2018; Kulkarni and Jagannadham, 2014; Kulkarni et al., 2014; Kulp and Kuehn, 2010). OMV-host interactions can benefit pathogens and contribute to their overall virulence strategy; however, host immune systems also detect OMVs and use them as signals to activate immune responses that improve the ability of the host to overcome infection (Kuehn and Kesty, 2005; Kaparakis-Liaskos and Ferrero, 2015; Ellis and Kuehn, 2010; Acevedo et al., 2014; Caruana and Walper, 2020).

Despite the extensive focus on interactions between bacterial OMVs and mammalian hosts, especially in the context of pathogenicity and disease, research is only beginning to uncover the role that OMVs play in the environment and, specifically, their role in interactions with plants. Because many tools are available to probe these interactions and many plant-microbe interaction mechanisms are already well-characterized, plant-pathogen interactions present an excellent opportunity to study the contributions of OMVs to bacterial virulence and OMV-mediated interkingdom communication.

Our current understanding of plant-pathogen interactions partly stems from a large body of work using the model host *Arabidopsis thaliana* and the model bacterial pathogen *Pseudomonas syringae* pv. *tomato* (*Pst*). *Pst* enters the leaf tissue through stomata or wounds in the leaf epithelium and proliferates in the intercellular space known as the apoplast (Katagiri et al., 2002; Xin and He, 2013). This stressful environment, which consists mostly of air and is devoid of nutrients and resources needed for bacterial growth (Xin and He, 2013), can be mimicked *in vitro* using minimal

media and has been shown to induce bacterial virulence factor expression (Lam et al., 2014). Plants detect invasion into the apoplast through a combination of extracellular and intracellular defense mechanisms and mount an immune response to clear the pathogen (Spoel and Dong, 2012; Jones and Dangl, 2006; Katagiri et al., 2002; Stael et al., 2015; Xin and He, 2013).

Some non-pathogens, including *P. fluorescens*, also activate a subset of plant immune responses at low levels despite their inability to proliferate in foliar tissue (Alfano and Collmer, 2001; Bakker et al., 2007; Pieterse et al., 2014; Weller et al., 2012; Cheng et al., 2017; Haas and Défago, 2005; Iavicoli et al., 2003; Zamioudis and Pieterse, 2012). This low-level plant immune response does not inhibit plant growth significantly, and some of these non-pathogens have even been shown to promote plant growth (Sivasakthi et al., 2014; Santoyo et al., 2012; Glick, 2012). A key difference between non-pathogenic commensals and pathogenic bacteria, specifically between *P. fluorescens* and *P. syringae*, is the ability of pathogens to overcome plant defenses using the type III secretion system (T3SS) (Deslandes and Rivas, 2012; Feng and Zhou, 2012; Gassmann and Bhattacharjee, 2012; Guo et al., 2009; Mazurier et al., 2015; Büttner and He, 2009). While T3SS studies have been instrumental in identifying and defining the complex pathways in plant innate immune responses, many other bacterial secretion pathways also play a role in plant-microbe interactions (Xin and He, 2013; Lomovatskaya and Romanenko, 2020).

Local immune responses to both pathogens and non-pathogens can lead to systemic immune protection in plants (Pieterse et al., 2014). Pathogenic bacteria often induce host expression of the isochorismate synthase 1 (*ICS1*) gene, which encodes an enzyme that catalyzes the production of salicylic acid (SA), a plant immune signal for systemic acquired resistance (Wildermuth et al., 2001; Glazebrook, 2005; Friedrich et al., 1995; Delaney et al., 1995; Cao et al., 1994; Lawton et al., 1996). For non-pathogens, it is widely believed that immune activation is triggered by pathogen-/microbe-associated molecular patterns (PAMPs/MAMPs) and that systemic immune induction occurs via SA-independent pathways (Pieterse et al., 2014). In addition to MAMPs, studies have revealed specific antibiotic, metabolite, and lipoprotein production in *P. fluorescens* strains that elicit local and systemic plant immune responses (Weller et al., 2012; Iavicoli et al., 2003; Tran et al., 2007; Maurhofer et al., 1994).

Our growing understanding of virulence in plant pathogenic bacteria has recently expanded to include OMV-mediated secretion and cargo delivery. Proteomic studies have revealed that OMVs from plant pathogenic bacteria contain plant cell-wall-degrading enzymes, components of protein secretion machinery and effectors, nucleic acids known to induce plant immune responses, and a variety of virulence factors (Kulkarni et al., 2015; Sidhu et al., 2008; Solé et al., 2015; Chowdhury and Jagannadham, 2013). OMVs from *Xanthomonas campestris* pv. *vesicatoria, X. campestris* pv. *campestris*, and *X. oryzae* pv. *oryzae* and virulence factors purified from these OMVs have been shown to trigger immune responses in plants that include callose deposition, increased transcription of pattern recognition receptors, and reactive oxygen species release (Solé et al., 2015; Tayi et al., 2016; Bahar et al., 2016). In addition, OMVs from *Xylella fastidiosa* block bacterial cell attachment to xylem cell walls, allowing the bacteria to spread further and cause disease throughout the plant (Ionescu et al., 2014). While these studies reveal enticing initial support for OMV involvement in bacterial virulence and plant immune activation, they also bring to light many unanswered questions about how plants detect OMVs, which immune pathways OMVs activate, whether OMV-mediated plant immune responses lead to improved resistance against pathogen infection, how specific immune responses are to OMVs from a given species or pathovar, and whether OMVs from non-pathogens also induce plant immune responses. Furthermore, it remains unknown how OMVs may work in concert with the producing bacterial cell to further virulence or plant immune activation.

In this study, we show that upon exposure to bacterial OMVs, plants can mount a broad-spectrum immune response against bacterial and oomycete pathogens. This response is conserved for OMVs from a variety of bacterial species, although not all species, and includes a complex range of direct plant immune responses and indirect seedling growth inhibition. Studying these different responses provides unique insight into how plants differentiate between beneficial, commensal, and pathogenic bacterial interactions. Furthermore, our data reveal an exciting new use for OMVs as a tool to uncouple plant growth and defense activation, as well as signaling and immune outcome.

RESULTS

P. syringae and *P. fluorescens* OMVs

To evaluate OMV production, we isolated OMVs from *Pst* and *P. fluorescens* Migula ATCC 13525 (*Pf*) grown first in rich and then in minimal liquid media to early stationary phase (Figure S1A) according to previously developed methods (McBroom et al., 2006; Chutkan et al., 2013; Lam et al., 2014). Minimal media has been shown to modulate OMV production and induce virulence factor expression (Prados-Rosales et al., 2014; Keenan and Allardyce, 2000; Roier et al., 2016; Lam et al., 2014). We noted that while bacterial cell viability and density were lower in cultures shifted to minimal media compared to those that were mock shifted to complete media, membrane integrity was not compromised (Figures S1B–S1D), demonstrating that the cells did not die during the shift. We compared OMV production in complete media to production in minimal media by assessing total protein and lipid in the preparations. After controlling for cell growth and culture density, we found that shifting to the minimal media did not alter OMV production in *Pst* or *Pf* (Table S1; Figures S1E–S1H). Additional characterization by transmission electron microscopy revealed that OMVs produced in complete and minimal media have similar size distributions and morphology (Figures 1A and S1I–S1L). The size and morphology of *Pst* and *Pf* OMVs are consistent with those reported for OMVs from other bacterial species, with diameters of mainly 50–150 nm (Schwechheimer and Kuehn, 2015; Beveridge, 1999; Kulkarni et al., 2014; Chowdhury and Jagannadham, 2013).

OMV pre-treatment protects against *Pst* challenge

Given that OMVs elicit immune responses in mammalian systems (Kaparakis-Liaskos and Ferrero, 2015), and that prior

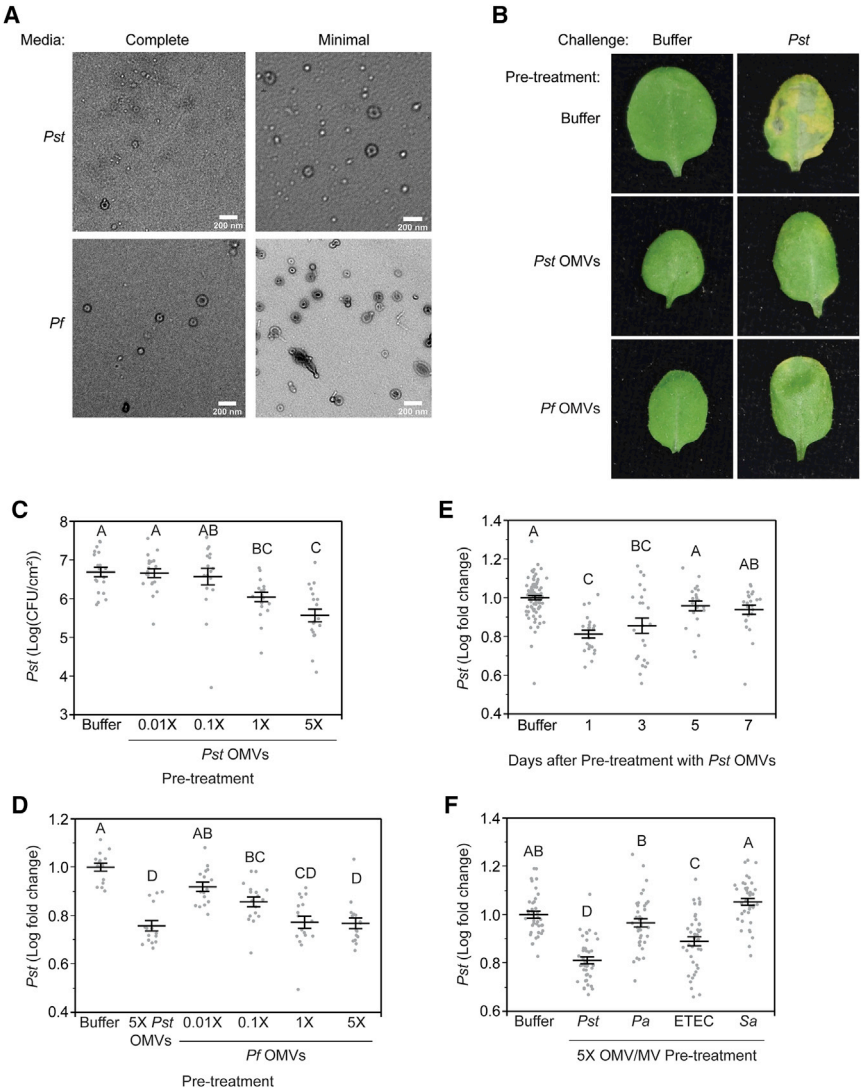

Figure 1. OMV pre-treatment protects against bacterial challenge

(A) TEM of OMVs isolated from *Pst* (top) or *Pf* (bottom) cultures grown in complete media (left) or shifted to minimal media for 2 h (right). Scale bar: 200 nm. Representatives from at least 15 images (*Pst* complete: n = 15; *Pst* minimal: n = 47; *Pf* complete: n = 26; *Pf* minimal: n = 35).

(B) Leaves infiltrated with either buffer (top) or OMVs from *Pst* (center) or *Pf* (bottom) cultures followed by challenge with either buffer (left) or *Pst* (right). OMVs were collected from minimal media cultures. Representative images from n = 7.

(C and D) *Pst* population size (C) or log fold change (D) in plants pre-treated with either buffer or various concentrations of *Pst* (C) or *Pf* (D) OMVs from minimal media cultures. Statistics: ANOVA, Tukey's honestly significant difference (HSD).

(E) *Pst* log fold change in plants pre-treated with 5× *Pst* OMVs from minimal media cultures. Leaves were pre-treated 1, 3, 5, or 7 days before challenge with *Pst*. Statistics: ANOVA, Tukey's HSD. Each treatment sample was normalized to a paired buffer-treated control.

(F) *Pst* log fold change in plants pre-treated with either buffer or OMVs/MVs from various species. Statistics: ANOVA, Tukey's HSD.

In (B)–(F), plants were pre-treated with OMVs, challenged with *Pst* 24 h later, and *Pst* CFU/cm^2 was measured after 4 days. In (C)–(F), n = 3 experimental replicates, each with at least 7 plants per treatment condition. Gray scatter points display the value from each plant tested. Horizontal line and error bars indicate means ± SEs; $p < 0.05$ in all of the statistical tests. Conditions not connected by the same letter are statistically significantly different.

See also Figures S1 and S2.

exposure to PAMPs enhances the plant immune response to a second challenge (Jung et al., 2009), we hypothesized that exposure to OMVs may have long-lasting immune implications for plants. To test whether OMVs protect against bacterial challenge, we treated *A. thaliana* leaves with OMVs pelleted from bacterial culture supernatants, waited 24 h, challenged leaves by infecting with *Pst*, and then measured bacterial population size after 4 days. Pre-treatment with *Pst* and *Pf* OMVs resulted in a complete rescue of leaf yellowing in response to *Pst* infection (Figures 1B and S2A). In response to increasing pre-treatment concentrations of OMVs from both *Pst* and *Pf*, we saw a corresponding decrease in bacterial population size 4 days post-challenge (Figures 1C and 1D). Importantly, pre-treatment with OMVs at both the 5× and 1× concentrations significantly reduced *Pst* growth at the day 4 time point (Figures 1C and 1D). We note that OMVs did not reduce *Pst* growth *in vitro* (Figure S2B), suggesting that this effect is not due to direct bacterial growth inhibition by the OMVs in the plant. In addition, the leaves remained protected from bacteria when challenged up to 3 days after pre-treatment with *Pst* OMVs (Figures 1E and S2C).

To determine whether the protective effect was due to OMVs rather than any proteins or other macromolecules that may co-pellet with OMVs from the culture supernatant, we purified the OMVs further using density gradient fractionation. Previous work from our lab has shown that this method separates OMVs from co-pelleted non-OMV-associated proteins and other secreted products (Horstman and Kuehn, 2000; Bauman and Kuehn, 2006). Based on protein and lipid content as well as the evaluation of fraction content by negative-staining electron microscopy, we determined that *Pst* OMVs were present in fractions 4–7 of the gradient (Figures 2A and S3A). When each fraction was used to pre-treat plants before bacterial challenge, we saw that only the fractions containing OMVs elicited protection against *Pst* (Figure 2B), which suggested that the protective response was in fact OMV-associated. Because no protective activity was found in fractions without OMVs, all subsequent

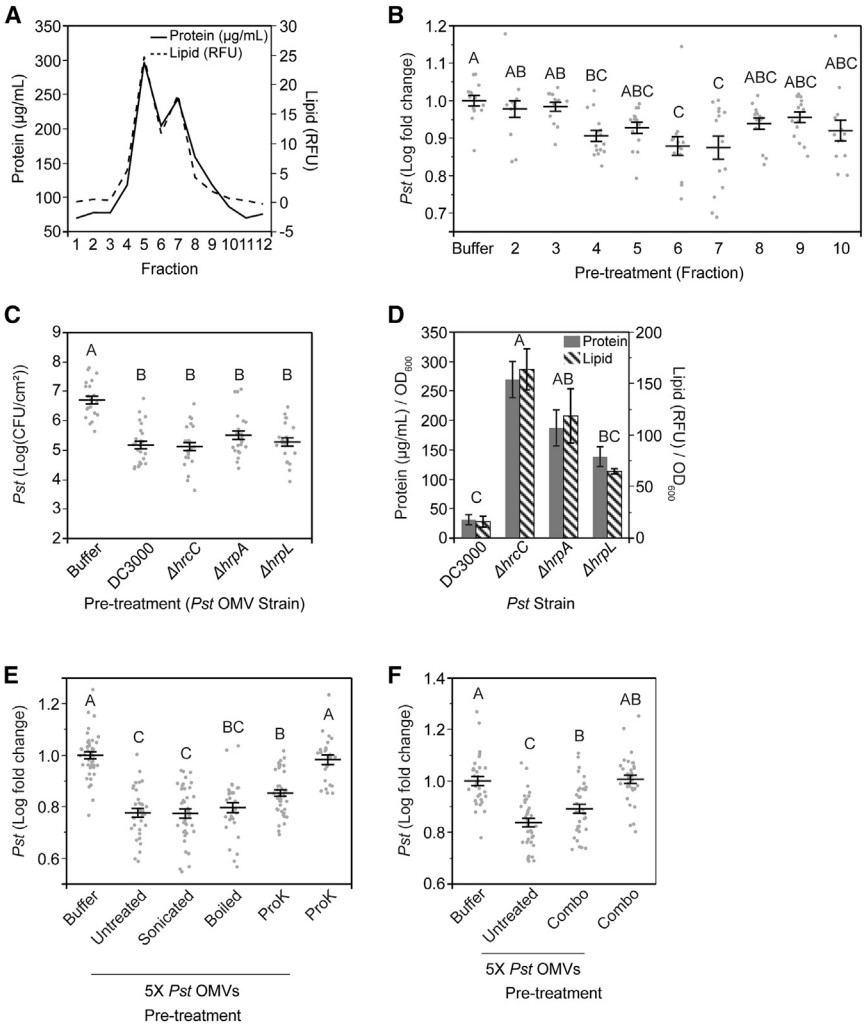

Figure 2. OMV-mediated protection is OMV-associated, type III secretion-independent, and withstands biochemical disruption

(A) OptiPrep density gradient with *Pst* OMVs showing distribution of protein and lipid across light (left) to heavy (right) fractions. Protein and lipid traces are representative of 3 experimental replicates.

(B) *Pst* log fold change in plants pre-treated with either buffer or various fractions from the density gradient in (A). Statistics: ANOVA, Tukey's HSD.

(C) *Pst* log fold change in plants pre-treated with either buffer or 5× *Pst* OMVs from WT, *ΔhrcC*, *ΔhrpA*, or *ΔhrpL*. Statistics: ANOVA, Tukey's HSD.

(D) OMV production as measured by protein and lipid normalized to culture density. Statistics: repeated-measures ANOVA, Tukey's HSD; n = 3.

(E) *Pst* log fold change in plants pre-treated with either buffer, 5× *Pst* OMVs, treated 5× *Pst* OMVs (sonicated, boiled, or treated with Proteinase K), or Proteinase K alone as a control. ProK: Proteinase K. Statistics: ANOVA, Tukey's HSD.

(F) *Pst* log fold change in plants pre-treated with either buffer, 5× *Pst* OMVs, 5× *Pst* OMVs exposed to a combination (Combo) of treatments, or the combination treatment alone as a control. Statistics: ANOVA, Tukey's HSD.

In (B), (C), (E), and (F), plants were pre-treated with OMVs, challenged with *Pst* 24 h later, and *Pst* colony-forming units (CFUs)/cm^2 were measured after 4 days. In (B), (C), (E), and (F), n = 3 experimental replicates, each with at least 7 plants per treatment condition. Gray scatter points display the value from each plant tested. Horizontal line and error bars indicate means ± SEs; $p < 0.05$ in all statistical tests. Conditions not connected by the same letter are statistically significantly different.

All OMVs were isolated from cultures grown in complete media and shifted to minimal media for 2 h.

See also Figure S3.

experiments could be performed using OMVs pelleted from culture supernatants without density gradient purification.

Plant immune responses to bacterial infection have been found to depend in part on plant recognition of bacterial T3SS effector-mediated modifications of plant proteins (Spoel and Dong, 2012; Jones and Dangl, 2006). As both effectors and components of the T3SS machinery have been identified in association with OMVs (Kulkarni et al., 2015), we wanted to test whether OMV-mediated protection and implied immune activation was dependent on T3SS factors. We used three well-studied T3SS mutants, *ΔhrcC*, *ΔhrpA*, and *ΔhrpL*, all of which eliminate the ability of *Pst* to induce leaf collapse and effector-triggered immune responses (Büttner and He, 2009; Roine et al., 1997; Deng et al., 1998; Fouts et al., 2002; Shen and Keen, 1993; Pirhonen et al., 1996; Gopalan et al., 1996; Lindgren et al., 1986). The *ΔhrcC* mutant lacks a core component of the machinery inserted into the bacterial outer membrane, while *ΔhrpA* lacks the pilus protein required to form the needle structure (Deng et al., 1998; Roine et al., 1997). In contrast, *ΔhrpL* lacks a sigma protein required for the coordinated expression of various components of the T3SS apparatus and effector proteins; therefore, OMVs from *ΔhrpL* should not contain effectors (Fouts et al., 2002; Shen and Keen, 1993). In response to pre-treatment with OMVs from any of the three T3SS mutant strains, we saw no reduction in protective responses as measured by the bacterial challenge assay (Figure 2C), indicating that T3SS effectors were not responsible for triggering protective immunity. Interestingly, while the *in vitro* growth of the three mutant strains did not differ from that of wild type (WT), all three mutants produced significantly more OMVs than WT (Figures 2D and S3B).

We next tested whether OMV-mediated protection was at all protein dependent. Interestingly, treating OMVs with proteinase K or boiling only slightly reduced their protective effect (Figure 2E). In fact, even using a combination of many different biochemical and physical treatments resulted only in slightly reduced protection against bacterial challenge (Figure 2F). For this combined treatment, polymyxin was used to interfere with lipopolysaccharide (LPS)-mediated immune interactions (Domingues et al., 2012; Cooperstock and Riegle, 1981), sonication was used to disrupt the OMV structure further before treating

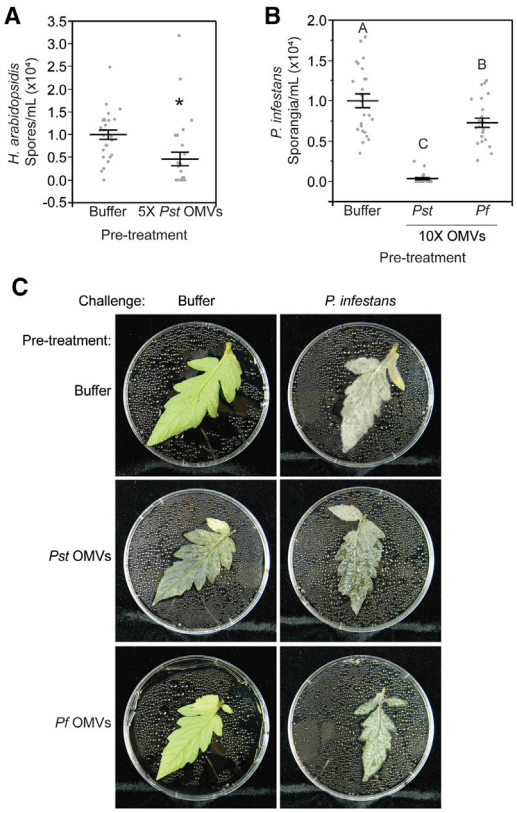

Figure 3. *Pst* and *Pf* OMVs protect against oomycete challenge in multiple plant species

(A) *Hyaloperonospora arabidopsidis* spore count in samples isolated from *A. thaliana* seedlings pre-treated with either buffer or 5× *Pst* OMVs. Statistics: 2-tailed Student's t test.

(B) *Phytophthora infestans* sporangia count in samples isolated from detached tomato leaves pre-treated with either buffer, 10× *Pst* OMVs, or 10× *Pf* OMVs. Statistics: ANOVA, Tukey's HSD.

(C) Tomato leaves pre-treated with buffer (top), *Pst* OMVs (center), or *Pf* OMVs (bottom) and challenged with buffer (left) or *Phytophthora infestans* (right). Representative images from n = 3 experimental replicates, each with 8 leaves per treatment condition.

In (A) and (B), n = 3 experimental replicates, each with at least 7 plants per treatment condition. Gray scatter points display the value from each plant tested. Horizontal line and error bars indicate means ± SEs; $p < 0.05$ in all statistical tests. Asterisk indicates statistical significance. Conditions not connected by the same letter are statistically significantly different.

All OMVs were isolated from cultures grown in complete media and shifted to minimal media for 2 h.

See also Figure S4.

with benzonase to digest nucleic acid, proteinase K treatment was used to digest any OMV-associated proteins, and boiling for 2 h in the presence of the detergent Tween 20 was used to disrupt lipid interactions and denature any remaining polypeptides. As shown by SDS-PAGE and agarose gel electrophoresis, no detectable proteins or nucleic acids remained in these treated OMV samples (Figures S3C–S3E). That this combination resulted in only a slight reduction in protection suggests that protein is not driving OMV-mediated protection against bacterial infection. It also suggests that the OMV-associated molecules leading to protection are highly stable, potentially implicating metabolites, lipids, and small protein epitopes, among other molecules.

Pst and *Pf* OMVs protect against oomycete challenge in multiple plant species

To explore how broadly OMV-mediated responses were able to protect against pathogens, we tested their effect on oomycete pathogenesis. *Hyaloperonospora arabidopsidis* is a well-studied biotrophic pathogen that requires a living host to grow and reproduce (Xin and He, 2013; Coates and Beynon, 2010; Mcdowell, 2014; Kamoun et al., 2015). In *A. thaliana*, pre-treatment with *Pst* OMVs led to a reduction in oomycete growth upon subsequent challenge (Figure 3A).

In tomato and potato, another well-studied oomycete pathogen, *Phytophthora infestans*, causes devastating disease and crop loss each year (Fry et al., 2015; Kamoun et al., 2015; Ristaino et al., 2019). To test whether bacterial OMVs protect against *P. infestans* infection in its natural host, we pre-treated detached tomato leaves of a susceptible cultivar (cv. Mountain Fresh Plus) with *Pst* OMVs, *Pf* OMVs, or a buffer control via vacuum infiltration. Interestingly, pre-treatment with *Pst* and *Pf* OMVs reduced sporangia counts after *P. infestans* challenge (Figures 3B, 3C, and S4A). These data suggest that bacterial OMVs are able to induce protective plant responses that improve plant disease resistance during bacterial and oomycete challenge. We note that while pre-treatment with *Pst* OMVs did lead to the reduced growth of *P. infestans* in the tomato, *Pst* OMV treatment also led to an interesting water-soaking phenotype that was not observed upon treatment with *Pf* OMVs (Figures 3C and S4A). *Pst* OMV-mediated water soaking was not observed in *A. thaliana* (Figure 1B), although *Pst* bacteria cause water soaking in both tomato and *A. thaliana* (Xin et al., 2016). These results lead us to speculate that, as a natural pathogen of tomato, *Pst* may secrete OMVs containing reactive cargo specifically targeting the host response pathways of tomato.

Biochemical and genetic characterization of OMV-mediated growth inhibition

Mounting an immune response requires plants to redirect their resources from growth to defense, resulting in growth inhibition (Albrecht and Argueso, 2017; Lozano-Durán and Zipfel, 2015; Hammoudi et al., 2018; Fan et al., 2014; Huot et al., 2014). Therefore, we hypothesized that OMV treatment would result in growth inhibition as a consequence of the implied immune activation that leads to protection. To test this hypothesis, we treated *A. thaliana* seedlings with increasing doses of *Pst* and *Pf* OMVs and observed *Pst* and *Pf* OMV dose-dependent seedling growth inhibition as measured by seedling weight (Figures 4A, 4B, and S5A–S5C). OMVs purified on a density gradient also inhibited seedling growth, thereby confirming that the growth inhibition activity was OMV-associated (Figure S5D), and growth was inhibited to a level similar to that of the commonly used PAMP flg22 (Figure S5E). Notably, *Pf* OMVs inhibited seedling growth even at extraordinarily low concentrations (Figures 4B and S5C). These results further support the concept that plants mount an immune response to OMVs.

Using growth inhibition as a convenient and sensitive assay to indicate immune induction, we set out to reveal which components of the OMVs were responsible for the protective

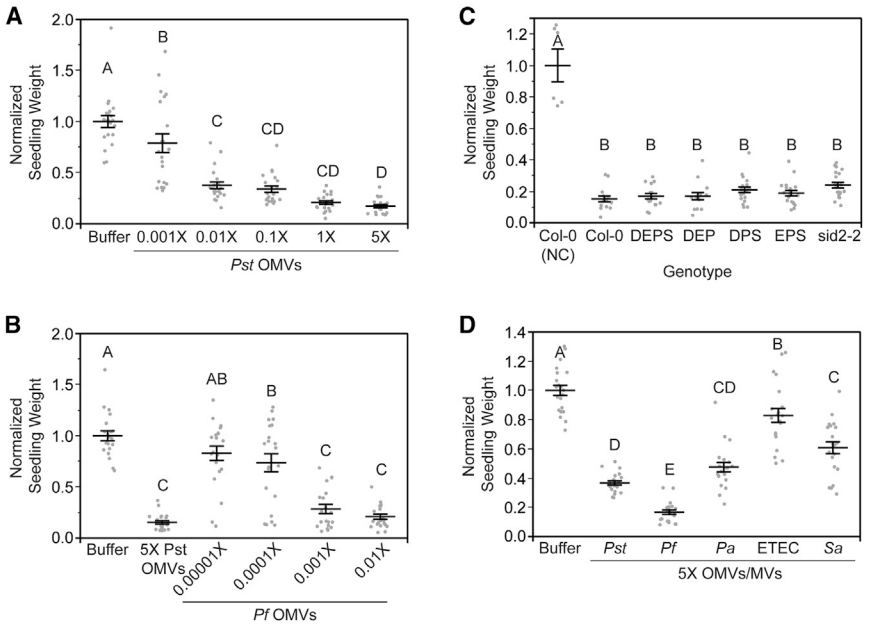

Figure 4. OMV treatment leads to seedling growth inhibition

(A and B) Seedling weight 7 days post-treatment with either buffer or various concentrations of *Pst* (A) or *Pf* (B) OMVs. Statistics: ANOVA, Tukey's HSD.

(C) Hormone mutant seedling weight 7 days post-treatment with 5× *Pst* OMVs. DEPS: *dde2-2/ein2-1/pad4-1/sid2-2*; DEP: *dde2-2/ein2-1/pad4-1*; DPS: *dde2-2/pad4-1/sid2-2*; and EPS: *ein2-1/pad4-1/sid2-2*. Statistics: ANOVA, Tukey's HSD.

(D) Seedling weight 7 days post-treatment with either buffer or OMVs/MVs from a variety of bacteria. Statistics: ANOVA, Tukey's HSD.

Pst and *Pf* OMVs were isolated from cultures grown in complete media and shifted to minimal media for 2 h. n = 3 experimental replicates, each with at least 7 plants per treatment condition. Gray scatter points display the value from each plant tested. Horizontal line and error bars indicate means ± SEs; $p < 0.05$ in all statistical tests. Conditions not connected by the same letter are statistically significantly different.

See also Figures S5 and S6.

activities and whether protection by different types of OMVs was mediated in the same manner. We applied various biochemical and physical treatments to the different OMV preparations and examined their effects on growth inhibition. Whereas disrupting OMV structure by sonication did not alter the growth inhibition phenotype, boiling and proteinase K reduced growth inhibition to the level of the buffer-treated control (Table 1; Figures S5F, S5G, S5J, S6A, S6B, S6F, S6G, and S6I). Interestingly, freeze-drying and salt stripping disrupted the growth phenotype of *Pst* OMVs but not of *Pf* OMVs isolated from minimal media, indicating that despite their similar overall ability to inhibit seedling growth, these OMVs differ in their active cargo composition and/or how those active cargo are associated with the OMVs (Table 1; Figures S5F, S5H, S6F, and S6H). The growth-inhibiting activity of *Pst* OMVs from complete media was surprisingly unperturbed by freeze-drying but was disrupted by salt stripping (Table 1; Figures S6C and S6D). Similarly, growth inhibition by *Pf* OMVs from complete media remained intact after freeze-drying (Table 1; Figure S6A). In notable contrast to the results from the bacterial challenge assays, which showed that protection was protein independent, these results suggest that seedling growth inhibition is modulated by OMV-associated proteins.

We further analyzed whether plant defense hormone signaling was involved in OMV-induced growth inhibition. As described previously, abolishing the jasmonic acid, SA, ethylene, and SA-independent *pad4* hormone pathways severely compromises plant immune responses (Tsuda et al., 2009). We discovered that OMVs inhibited seedling growth in plants lacking all of these hormone pathways (Figure 4C). Slight growth differences between the hormone mutants and WT seedlings were accounted for in analyzing these data (Figure S6L). These results suggest that neither jasmonic acid, SA, ethylene, nor *pad4* signaling is required for OMV-mediated growth inhibition.

Bacterial OMVs induce plant *ICS1* expression involved in SA biosynthesis

To assess the plant immune response to OMVs, we used *A. thaliana* plants containing a luciferase reporter fused to the *ICS1* gene promoter. Plants infiltrated with *Pst* OMVs showed induced *ICS1* expression, while those treated with *Pf* OMVs did not (Figures 5A–5D and S7A). In comparison with bacterial cell-induced *ICS1* expression, we noted that *Pst* OMVs induced longer lasting but less robust *ICS1* expression (Figures 5A–5D and S7A). To confirm that the induced *ICS1* leads to SA accumulation in response to *Pst* OMV treatment, we quantified its production using high-performance liquid chromatography (HPLC). Compared to the buffer-treated control, *Pst* OMVs led to increased accumulation of both stored and free forms of SA (SAG and SA) (Figures 5E, 5F, and S7B). Together, *ICS1* expression and corresponding SA accumulation, or lack thereof, suggest that OMVs induce a variety of hormone-dependent and -independent plant immune responses and reveal key differences in immune activation by OMVs from pathogenic versus beneficial bacteria.

Similar to the apoplast environment, minimal media induces the expression of bacterial virulence factors (Lam et al., 2014). We hypothesized that even though minimal media does not affect OMV production (Table S1; Figures S1E–S1H), it may influence host reactivity, as has been shown in mammalian systems (Orench-Rivera and Kuehn, 2016; Kulkarni et al., 2014; Ellis and Kuehn, 2010). OMVs isolated from minimal media cultures may contain more host-reactive cargo than those isolated from complete media cultures and would activate stronger immune responses when used to treat plants. However, we found that OMVs isolated from minimal media cultures did not induce significantly stronger or qualitatively different *ICS1* responses than OMVs isolated from complete media (Figures 5A–5D and S7A).

In addition to *ICS1* expression, we found that bacterial OMVs could activate mitogen-activated protein kinase (MAPK)

Table 1. Summary of growth inhibition and bacterial protection phenotypes in response to treatment or pre-treatment with OMVs

	Growth inhibition?[a]				Bacterial protection?[a]
Treatment	*Pst* C	*Pst* M	*Pf* C	*Pf* M	*Pst* M
Sonication	Y	Y	Y	Y	Y
Salt strip (NaCl)	N[b]	N[b]	Y[b]	Y[b]	–
UV (30 min)	N	N	N	N	–
Frozen in LN_2 and lyophilized	Y	N	Y	Y	–
Boiled (100°C, 2 hr)	N	N	N	N	Y
Proteinase K (100 μM, 1 h, 37°C)	N	N	N	N	Y/N
Combined (polymyxin, sonicate, benzonase, Proteinase K, Tween 20, boil)	N	N	Y/N[c]	N	Y/N[c]
Organic extraction (MeOH and DCM)	Y/N[d]	–	–	–	–
Size exclusion on extraction pellet	Y/N[e]	–	–	–	–

See also Figures 2E, 2F, S5, and S6.

[a]Seedlings (for growth inhibition) or 3-week-old plants (for bacterial protection) were treated with OMVs from the indicated strain and condition. OMVs were treated before application with the indicated biochemical or physical stressors. C: OMVs isolated from complete media; M: OMVs isolated from minimal media; Y: activity retained in OMVs; N: activity reduced to level of buffer-treated control; Y/N: activity reduced to a level between OMVs and buffer-treated control. –: activity not tested for these conditions.

[b]Activity was also assessed for post-treatment supernatants and activity was detected in supernatant.

[c]Activity was <5× *Pst* OMVs and greater than buffer control, but not statistically different from the negative control with treatments alone.

[d]Activity was reduced compared to unfractionated 5× *Pst* OMVs but retained in both fractions.

[e]Activity was reduced compared to unfractionated 5× *Pst* OMV extraction pellet, but only in the fraction containing components larger than 10 kDa.

phosphorylation known to be involved in PAMP-triggered immune signaling (Figures 5G, 5H, and S8A) (Tsuda et al., 2013). However, compared to the well-characterized PAMP signaling elicited by flg22, OMV-induced MAPK phosphorylation lasted much longer, suggesting that OMVs might activate different, likely more complex, plant immune responses than a single PAMP signal. Further support for a break from classical PAMP- or effector-triggered immune responses comes from observing the leaf phenotypes upon infiltration with OMVs. Despite activating plant immune responses, OMV infiltration did not lead to water soaking, leaf yellowing, or collapse in *A. thaliana* (Figures 5I and S8B). These results suggest that *A. thaliana* detects OMVs and mounts immune responses distinct from either the canonical PAMP- or the effector-triggered immune responses, and that *A. thaliana* modulates immune output upon distinguishing OMVs from pathogenic versus beneficial bacteria.

OMVs from diverse bacteria modulate plant immune responses

To determine whether immune activity and growth inhibition were unique to vesicles derived from model plant bacteria, we isolated OMVs from Gram-negative bacteria *P. aeruginosa* (*Pa*) and enterotoxigenic *Escherichia coli* (ETEC), and membrane vesicles (MVs) from the Gram-positive *Staphylococcus aureus* (*Sa*). We then pre-treated leaves with these OMVs/MVs and measured various immune responses or protection against *Pst* challenge. While none of these OMVs/MVs induced *ICS1* expression, OMVs from *Pa*, and to a lesser extent, OMVs from ETEC and MVs from *Sa* did lead to plant growth inhibition (Table 2; Figures 4D, 5J, and 5K). Interestingly, ETEC OMVs also elicited responses that protected against *Pst* challenge, despite different immune modulation than was observed for *Pst* and *Pf* OMVs (Table 2; Figure 1F). These results suggest that protective immune induction in plants is not limited to OMVs from plant-associated bacteria, and that there is cross-species protection in response to OMVs from a variety of bacteria.

DISCUSSION

Our study shows for the first time that bacterial OMVs elicit plant immune responses that protect against future bacterial and oomycete challenge. Furthermore, the biological activities in fractions of mechanically and biochemically disrupted OMVs point to species- and media-dependent differences in cargo exported by the OMVs. These data are consistent with the concept that OMVs carry complex mixtures of immunomodulatory factors that collectively contribute to differential plant responses to bacterial pathogens and beneficial bacteria. Our findings provide novel insights into SA-independent immune pathways and growth-defense trade-offs and reveal a new layer of complexity in plant-pathogen interactions.

The concept that bacteria release OMVs that activate antibacterial immune responses may seem counterproductive. However, it should be noted that a parallel situation exists for mammalian bacterial pathogens where a cost-benefit trade-off is evident. In these cases, bacterial OMVs are known to elicit strong innate immune responses in mammalian hosts and also harbor highly antigenic epitopes and adjuvanticity that evoke protective and long-term immunity toward the pathogen generating the OMVs (Kuehn and Kesty, 2005; Kaparakis-Liaskos and Ferrero, 2015; Ellis and Kuehn, 2010; Acevedo et al., 2014; Caruana and Walper, 2020). Despite this, OMVs are used by bacteria to deliver toxins and other virulence determinants to the host and help the bacteria adapt to the hostile and antimicrobial host environment (Zingl et al., 2020; Chatterjee and Chaudhuri, 2011; Horstman and Kuehn, 2000; Kesty et al., 2004; Pauls-son et al., 2018). These studies reveal a critical artifact of most current reductionist experimental approaches that study how OMVs behave within hosts and interact with the host immune system: the removal of bacterial cells from the investigation. Experiments using highly purified OMVs are important in revealing their unique reactivity but have not been designed to address questions about how OMVs could work simultaneously and potentially synergistically with bacterial cells against the plant immune response. Therefore, although we observe that OMVs

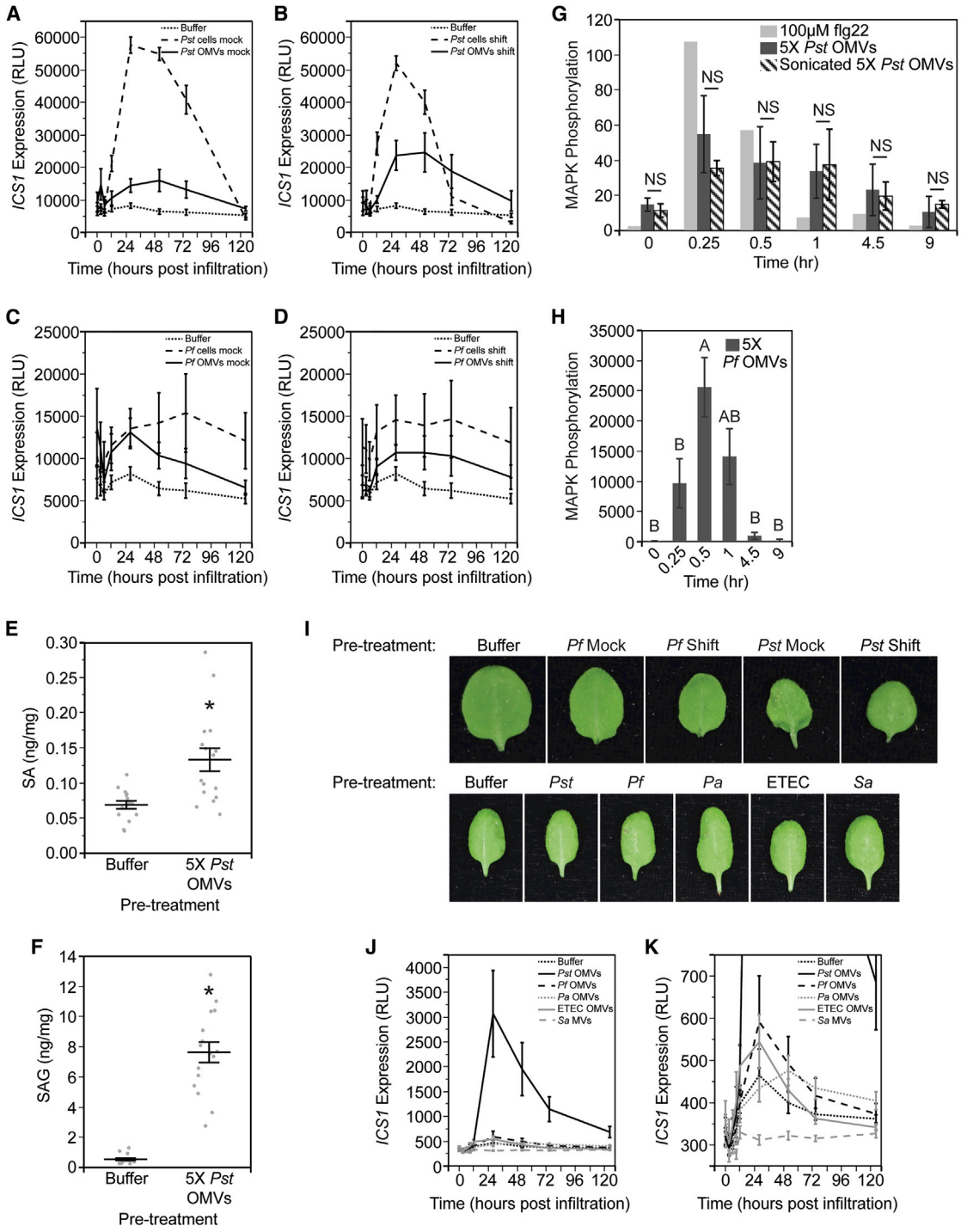

Figure 5. Bacterial OMVs induce plant *ICS1* expression involved in SA biosynthesis

(A–D) *ICS1* expression over time from Col-0 *ICS1*:LUC transgenic plants infiltrated with *Pst* cells or 5× *Pst* OMVs (A and B), or *Pf* cells or 5× *Pf* OMVs (C and D). Cells and OMVs were isolated from cultures grown in complete media and shifted to either (A and C) complete (mock) or (B and D) minimal (shift) media for 2 h. Statistics: repeated-measures ANOVA, ANOVA subdivided by time point.

(E and F) HPLC quantification of (E) salicylic acid (SA) and (F) SA 2-*O*-β-D-glucose (SAG) metabolites from leaves infiltrated with either a buffer control or 5× *Pst* OMVs from cultures shifted to minimal media for 2 h. Statistics: 2-tailed Student's t test.

(G and H) MAPK activation over time in response to treatment with flg22, 5× *Pst* OMVs, or sonicated 5× *Pst* OMVs (G), or 5× *Pf* OMVs (H). Statistics: (G) repeated-measures ANOVA, 2-tailed Student's t test after subdivision by time point; (H) ANOVA, Tukey's HSD. 5× *Pst* OMVs treatment: n = 5; sonicated 5× *Pst* OMVs treatment: n = 3; 5× *Pf* OMVs treatment: n = 3.

(legend continued on next page)

Table 2. Summary of plant immune activation by OMVs/MVs from different bacterial species

	Genus/species[a]				
	Pst	*Pf*	*Pa*	ETEC	*Sa*
Visible phenotype?	N	N	N	N	N[b]
Induces *ICS1*?	Y	N	N	N	N
Leads to SA accumulation	Y	–	–	–	–
Stunts seedling growth?	Y	Y	Y	Y[c]	Y[c]
Differential MAPK phosphorylation?	Y	Y	–	–	–
Protects against bacterial challenge?	Y	Y	N	Y	N
Protects against *H. arabidopsidis* challenge?	Y	Y	–	–	–
Protects against *P. infestans* challenge?	Y[d]	Y	–	–	–

See also Figures 1, 3, 4, 5, S4, S7, and S8.

[a]OMVs/MVs were isolated from the indicated species and applied to plants. Immune activity was measured using a variety of assays. Y: activity present in OMVs/MVs; N: activity absent in OMVs/MVs; –: activity not tested for these conditions.

[b]Water-soaking phenotype observed in 3-week-old plants at 1 h post-infiltration but returned to normal plant physiology by 3 h post-infiltration.

[c]Seedling growth was stunted to a level between that of buffer and 5× *Pst* OMVs.

[d]Pre-treatment with Pst OMVs induced significant water soaking, possibly destroying leaf tissue and thereby preventing *P. infestans* growth.

elicit antibacterial, protective plant responses, we are likely missing their contribution to bacterial virulence by eliminating synergistic interactions with bacterial cells. Untangling the nuances of how vesicles produced by bacteria contribute to the plant immune response during the various stages of infection is a worthwhile topic for future study and will shed light on a previously unappreciated layer of interaction during natural pathogenesis.

The type of immune responses elicited by the various OMV preparations are unique but reveal insights when compared to those activated by PAMPs. Although both *Pst* and *Pf* OMVs led to protection against bacterial and oomycete challenge (Figures 1C, 1D, 3A, 3B, S2A, and S4A), *Pf* OMVs did so independently of *ICS1* expression (Figures 5C, 5D, and S7A; Table 2). The lack of *ICS1* induction, and subsequently SA accumulation, is consistent with reports of induced systemic resistance by beneficial microbes, which is thought to be mediated by MAMPs (Pieterse et al., 2014; Bakker et al., 2007). The *ICS1* induction time course triggered by *Pst* OMVs is very similar to that of a PAMP-triggered response (Tsuda et al., 2008; Thilmony et al., 2006; Nomura et al., 2012; Jung et al., 2009). This suggests that the immune activation in response to both *Pst* and *Pf* OMVs was in response to PAMPs/MAMPs or other immune-active molecules contained in or on the OMVs, but also suggests key differences between *Pst* and *Pf* OMVs in the exact molecule(s) responsible for protection and in activation pathways. It is important to note that while OMV-mediated immune responses in both *A. thaliana* and tomato resemble those that activate systemic immune responses in plants, systemic protection against *Pst*, *H. arabidopsidis*, or *P. infestans* was not tested in our assays.

Despite many similarities to PAMP/MAMP-induced signaling in plants, our data also reveal distinct immune activation. For example, our results show that OMVs induce longer MAPK activation than a well-studied PAMP elicitor, flg22 (Figures 5G and 5H). Prolonged MAPK activation has been shown to play a critical role in altering defense-related photosynthetic activities and is also essential to robust effector-triggered immune responses (Su et al., 2018). This suggests that OMVs may be activating a unique combination of typically PAMP/MAMP-associated and effector-associated plant immune programs.

In addition, our data demonstrate that neither the T3SS machinery nor the effectors are responsible for OMV-mediated protective immune responses. OMVs from all three T3SS mutants protected against bacterial challenge to the same level as OMVs from WT (Figure 2C). The results using *ΔhrpL* OMVs, which should contain no known effectors, were particularly surprising because effectors have been identified in OMVs from plant pathogens, and some of them are known to be potent immune activators (Kulkarni et al., 2014, 2015; Sidhu et al., 2008; Solé et al., 2015; Chowdhury and Jagannadham, 2013; Fouts et al., 2002; Shen and Keen, 1993). It is also of interest that all of the T3SS mutants produced significantly more OMVs than WT (Figures 2D and S3B), which could be due to fewer connections between the inner and outer membrane, an envelope characteristic found previously to affect OMV production (Schwechheimer et al., 2014, 2015; Bernadac et al., 1998; Suzuki et al., 1978; Yem and Wu, 1978).

We were also intrigued by the observation that the protective effect was independent of OMV-associated proteins (Figures 2E, 2F, S3C, and S3D), while, in contrast, growth inhibition depended on protein cargo (Table 1; Figures S5F, S5G, S5I, S6A, S6B, S6G, S6I, and S6K). The long incubation with Proteinase K likely led not only to the digestion of all OMV-associated proteins but also integral membrane proteins, allowing the enzyme to access the OMV lumen and degrade remaining proteins, as evidenced by a lack of detectable protein bands in an SDS-PAGE gel (Figures S3C and S3D). As a result, these data suggested to us that the *Pst* OMV components that elicit protection

(I) Images of infiltrated leaves showing no disease phenotype or water soaking in *A. thaliana* in association with the infiltration of OMVs/MVs from any of the species tested. Representative images from n = 2, each with 6 leaves per treatment condition.

(J) *ICS1* expression over time from Col-0 *ICS1*:LUC transgenic plants infiltrated with OMVs/MVs from various species. Statistics: repeated-measures ANOVA, ANOVA subdivided by time point.

(K) Magnified graph from (J) showing differences in *ICS1* expression among all OMV/MV treatments except *Pst*.

In (A)–(F) and (J) and (K), n = 3 experimental replicates, each with at least 7 plants per treatment condition. Gray scatter points display the value from each plant tested. Horizontal line and error bars indicate means ± SEs; $p < 0.05$ in all statistical tests. Asterisks indicate statistical significance. Conditions not connected by the same letter are statistically significantly different.

See also Figures S7 and S8.

are lipids, small molecules, carbohydrates, and/or other molecules (Figures 2E, 2F, S3C, and S3D). Although proteinaceous bacterial effectors are frequently studied for their ability to elicit plant immune responses, many non-protein elicitors have also been characterized (Silipo et al., 2010, Morgunov et al., 2017; Erbs and Newman, 2012; Ranf, 2016). Because *Pst* and *Pf* OMV-mediated growth inhibition was highly sensitive to treatment with Proteinase K or boiling (Table 1; Figures S5F, S5G, S5I, S6A, S6B, S6G, S6I, and S6K), while protection was largely protein independent (Figures 2E, 2F, S3C, and S3D), these results uncouple growth inhibition from immune activation and protection and thereby reveal a novel use for OMVs to probe the trade-offs between plant growth and defense. Further studies to isolate the distinct immune elicitors found in OMVs are needed and will likely uncover new aspects of plant immunity.

Growth-inhibition experiments revealed substantial differences between *Pst* and *Pf* OMV-mediated plant interaction. Most strikingly, *Pf* OMVs led to much more potent growth inhibition than *Pst* OMVs, as shown by their ability to inhibit seedling growth at a 10-fold lower dose (Figures 4A, 4B, and S5A–S5C). This was surprising since many strains of fluorescent pseudomonads are known to promote plant growth (Bakker et al., 2007; Iavicoli et al., 2003, Sivasakthi et al., 2014); however, it should also be noted that many of these strains promote plant growth either by helping the plant obtain critical nutrients or by suppressing disease-causing microbes (Berg, 2009; Haas and Défago, 2005; Loper et al., 2007; Glick, 2012).

Various biochemical treatments differentially affected the activity of OMV preparations from different strains and conditions, further supporting our hypothesis that these OMVs consist of distinct cargo (Table 1; Figures S5F–S5J, and S6A–S6K). For example, flash-freezing, which could disrupt or damage proteins involved in modulating plant responses, eliminated the growth-inhibition phenotype in *Pst* OMVs from minimal media but had no effect on *Pst* OMVs from complete media (Table 1; Figures S5F and S6C). Intriguingly, flash-freezing also had no effect on *Pf* OMVs from minimal media (Table 1; Figure S6F). This difference in sensitivity implies that the OMV component(s) responsible for mediating growth inhibition differ(s) between the various species and conditions, and suggests that in nutrient-rich conditions, when virulence factor expression is low, *Pst* OMVs contain cargo similar to that secreted by a beneficial bacterium.

Bacterial OMVs have a wide array of functions in mammalian studies and have been exploited for human benefit through their use in vaccines. Here, we show that OMVs could have similarly beneficial applications in plant systems and have laid the groundwork for future experimentation by demonstrating that OMVs elicit plant immune responses that protect against bacterial and oomycete challenge. Of particular interest, our results reveal novel differences between bacterial pathogen-mediated and beneficial bacterial-mediated immune activation and OMV packaging, provide a new tool for probing SA-independent immune pathways and growth-defense trade-offs, and uncover new aspects of OMV-mediated interkingdom communication. By activating numerous pathways, OMVs elicit a complex immune response that would be difficult for pathogens to adapt to and overcome, which supports a role for bacterial OMVs in agricultural applications to promote durable resistance. While many experiments are needed to determine the precise mechanisms of OMV-mediated plant immune activation, a particularly pressing future direction is to determine the OMV-associated molecule or set of molecules responsible for plant immune activation. In summary, this work provides new perspectives on the complexity of plant-bacteria interactions and differences in interkingdom communication and immune activation by pathogenic versus beneficial bacteria, which will be critically important in the development of new disease management techniques.

STAR★METHODS

Detailed methods are provided in the online version of this paper and include the following:

- KEY RESOURCES TABLE
- RESOURCE AVAILABILITY
  - Lead contact
  - Materials availability
  - Data and code availability
- EXPERIMENTAL MODEL AND SUBJECT DETAILS
  - Bacterial strains and culture conditions
  - Oomycete strains and propagation conditions
  - Plant lines and growth conditions
- METHOD DETAILS
  - Bacterial OMV/MV preparations
  - Sytox Green assay
  - TEM and negative staining
  - ICS1 expression
  - SA/SAG extraction and quantification
  - Seedling growth inhibition
  - Bacterial challenge
  - OMV disruption
  - MAPK activation
  - H. arabidopsidis challenge
  - P. infestans challenge
  - OMV organic extraction
  - Size exclusion fractionation
- QUANTIFICATION AND STATISTICAL ANALYSIS

SUPPLEMENTAL INFORMATION

Supplemental Information can be found online at https://doi.org/10.1016/j.celrep.2020.108645.

ACKNOWLEDGMENTS

We thank the Arabidopsis Biological Research Center for *dde2-2/ein2-1/pad4-1/sid2-2*, *dde2-2/ein2-1/pad4-1*, *dde2-2/pad4-1/sid2-2*, *ein2-1/pad4-1/sid2-2*, and *sid2-2* seeds; P. Zwack for assistance with the *H. arabidopsidis* experiments; A. Saville and J. Hansel for assistance with the *P. infestans* experiments; H. Yoo for help with the HPLC experiments; and M.G. Plue and the Duke University Shared Materials Instrument Facility (SMIF) for training and use of the transmission electron microscope. This material is based upon work supported by the National Science Foundation under grant no. 1931309. We also acknowledge support from the Duke SOM Core Voucher Program to M.J.K., the Duke University Medical Center, and grants from the National Institutes of Health (NIH) (1R35GM118036) and by the Howard Hughes Medical Institute and the Gordon and Betty Moore Foundation (through grant no. GBMF3032) to X.D. This work was performed in part at

the Duke University SMIF, a member of the North Carolina Research Triangle Nanotechnology Network (RTNN), which is supported by the National Science Foundation (grant no. ECCS-1542015) as part of the National Nanotechnology Coordinated Infrastructure (NNCI). A portion of the work on *P. infestans* was conducted at North Carolina State University, with support from the Kenan Institute of Engineering, Science, and Technology.

AUTHOR CONTRIBUTIONS

H.M.M and M.J.K designed the research. S.G.Z. designed and carried out the MAPK assays and *H. arabidopsidis* challenge experiments and provided substantial feedback on the overall research design. J.B.R. supervised and provided feedback on the experimentation with *P. infestans.* X.D. supervised the *A. thaliana* research, supplied feedback on the overall research design, and provided critical feedback on the manuscript. H.M.M. carried out all of the other experiments and statistical analysis and prepared the figures. H.M.M. and M.J.K. wrote the manuscript, with input from all of the authors.

DECLARATION OF INTERESTS

The authors declare no competing interests.

Received: July 8, 2020
Revised: October 26, 2020
Accepted: December 21, 2020
Published: January 19, 2021

REFERENCES

Acevedo, R., Fernández, S., Zayas, C., Acosta, A., Sarmiento, M.E., Ferro, V.A., Rosenqvist, E., Campa, C., Cardoso, D., Garcia, L., and Perez, J.L. (2014). Bacterial outer membrane vesicles and vaccine applications. Front. Immunol. *5*, 121.

Albrecht, T., and Argueso, C.T. (2017). Should I fight or should I grow now? The role of cytokinins in plant growth and immunity and in the growth-defence trade-off. Ann. Bot. *119*, 725–735.

Alfano, J.R., and Collmer, A. (2001). CHAPTER 5 - Mechanisms of Bacterial Pathogenesis in Plants: Familiar Foes in a Foreign Kingdom. In Principles of Bacterial Pathogenesis, E.A. Groisman, ed. (Academic Press).

Bahar, O., Mordukhovich, G., Luu, D.D., Schwessinger, B., Daudi, A., Jehle, A.K., Felix, G., and Ronald, P.C. (2016). Bacterial Outer Membrane Vesicles Induce Plant Immune Responses. Mol. Plant Microbe Interact. *29*, 374–384.

Bakker, P.A.H.M., Pieterse, C.M.J., and van Loon, L.C. (2007). Induced Systemic Resistance by Fluorescent Pseudomonas spp. Phytopathology *97*, 239–243.

Bauman, S.J., and Kuehn, M.J. (2006). Purification of outer membrane vesicles from Pseudomonas aeruginosa and their activation of an IL-8 response. Microbes Infect. *8*, 2400–2408.

Berg, G. (2009). Plant-microbe interactions promoting plant growth and health: perspectives for controlled use of microorganisms in agriculture. Appl. Microbiol. Biotechnol. *84*, 11–18.

Berleman, J., and Auer, M. (2013). The role of bacterial outer membrane vesicles for intra- and interspecies delivery. Environ. Microbiol. *15*, 347–354.

Bernadac, A., Gavioli, M., Lazzaroni, J.C., Raina, S., and Lloubès, R. (1998). Escherichia coli tol-pal mutants form outer membrane vesicles. J. Bacteriol. *180*, 4872–4878.

Beveridge, T.J. (1999). Structures of gram-negative cell walls and their derived membrane vesicles. J. Bacteriol. *181*, 4725–4733.

Blanco, F., Salinas, P., Cecchini, N.M., Jordana, X., Van Hummelen, P., Alvarez, M.E., and Holuigue, L. (2009). Early genomic responses to salicylic acid in Arabidopsis. Plant Mol. Biol. *70*, 79–102.

Bonnington, K.E., and Kuehn, M.J. (2016). Outer Membrane Vesicle Production Facilitates LPS Remodeling and Outer Membrane Maintenance in Salmonella during Environmental Transitions. MBio *7*, e01532–16.

Büttner, D., and He, S.Y. (2009). Type III protein secretion in plant pathogenic bacteria. Plant Physiol. *150*, 1656–1664.

Cao, H., Bowling, S.A., Gordon, A.S., and Dong, X. (1994). Characterization of an Arabidopsis Mutant That Is Nonresponsive to Inducers of Systemic Acquired Resistance. Plant Cell *6*, 1583–1592.

Caruana, J.C., and Walper, S.A. (2020). Bacterial Membrane Vesicles and Their Applications as Vaccines and in Biotechnology. In Bacterial Membrane Vesicles: Biogenesis, Functions and Applications, M. Kaparakis-Liaskos and T.A. Kufer, eds. (Springer).

Chatterjee, D., and Chaudhuri, K. (2011). Association of cholera toxin with Vibrio cholerae outer membrane vesicles which are internalized by human intestinal epithelial cells. FEBS Lett. *585*, 1357–1362.

Chaturvedi, R., Venables, B., Petros, R.A., Nalam, V., Li, M., Wang, X., Takemoto, L.J., and Shah, J. (2012). An abietane diterpenoid is a potent activator of systemic acquired resistance. Plant J. *71*, 161–172.

Cheng, X., Etalo, D.W., van de Mortel, J.E., Dekkers, E., Nguyen, L., Medema, M.H., and Raaijmakers, J.M. (2017). Genome-wide analysis of bacterial determinants of plant growth promotion and induced systemic resistance by Pseudomonas fluorescens. Environ. Microbiol. *19*, 4638–4656.

Chowdhury, C., and Jagannadham, M.V. (2013). Virulence factors are released in association with outer membrane vesicles of Pseudomonas syringae pv. tomato T1 during normal growth. Biochim. Biophys. Acta *1834*, 231–239.

Chutkan, H., Macdonald, I., Manning, A., and Kuehn, M.J. (2013). Quantitative and qualitative preparations of bacterial outer membrane vesicles. Methods Mol. Biol. *966*, 259–272.

Coates, M.E., and Beynon, J.L. (2010). Hyaloperonospora Arabidopsidis as a pathogen model. Annu. Rev. Phytopathol. *48*, 329–345.

Cooperstock, M., and Riegle, L. (1981). Polymyxin B inactivation of lipopolysaccharide in vaccines of Gram-negative bacteria. Infect. Immun. *33*, 315–318.

Delaney, T.P., Friedrich, L., and Ryals, J.A. (1995). Arabidopsis signal transduction mutant defective in chemically and biologically induced disease resistance. Proc. Natl. Acad. Sci. USA *92*, 6602–6606.

Dempsey, D.A., and Klessig, D.F. (2012). SOS - too many signals for systemic acquired resistance? Trends Plant Sci. *17*, 538–545.

Dempsey, D.A., and Klessig, D.F. (2017). How does the multifaceted plant hormone salicylic acid combat disease in plants and are similar mechanisms utilized in humans? BMC Biol. *15*, 23.

Deng, W.L., Preston, G., Collmer, A., Chang, C.J., and Huang, H.C. (1998). Characterization of the hrpC and hrpRS operons of Pseudomonas syringae pathovars syringae, tomato, and glycinea and analysis of the ability of hrpF, hrpG, hrcC, hrpT, and hrpV mutants to elicit the hypersensitive response and disease in plants. J. Bacteriol. *180*, 4523–4531.

Deslandes, L., and Rivas, S. (2012). Catch me if you can: bacterial effectors and plant targets. Trends Plant Sci. *17*, 644–655.

Domingues, M.M., Inácio, R.G., Raimundo, J.M., Martins, M., Castanho, M.A., and Santos, N.C. (2012). Biophysical characterization of polymyxin B interaction with LPS aggregates and membrane model systems. Biopolymers *98*, 338–344.

Ellis, T.N., and Kuehn, M.J. (2010). Virulence and immunomodulatory roles of bacterial outer membrane vesicles. Microbiol. Mol. Biol. Rev. *74*, 81–94.

Erbs, G., and Newman, M.-A. (2012). The role of lipopolysaccharide and peptidoglycan, two glycosylated bacterial microbe-associated molecular patterns (MAMPs), in plant innate immunity. Mol. Plant Pathol. *13*, 95–104.

Esoda, C.N., and Kuehn, M.J. (2019). *Pseudomonas aeruginosa* Leucine Aminopeptidase Influences Early Biofilm Composition and Structure via Vesicle-Associated Antibiofilm Activity. MBio *10*, e02548–19.

Fan, M., Bai, M.Y., Kim, J.G., Wang, T., Oh, E., Chen, L., Park, C.H., Son, S.H., Kim, S.K., Mudgett, M.B., and Wang, Z.Y. (2014). The bHLH transcription factor HBI1 mediates the trade-off between growth and pathogen-associated molecular pattern-triggered immunity in Arabidopsis. Plant Cell *26*, 828–841.

Feng, F., and Zhou, J.M. (2012). Plant-bacterial pathogen interactions mediated by type III effectors. Curr. Opin. Plant Biol. *15*, 469–476.

Florez, C., Raab, J.E., Cooke, A.C., and Schertzer, J.W. (2017). Membrane Distribution of the *Pseudomonas* Quinolone Signal Modulates Outer Membrane Vesicle Production in *Pseudomonas aeruginosa*. MBio *8*, e01034, e17.

Fouts, D.E., Abramovitch, R.B., Alfano, J.R., Baldo, A.M., Buell, C.R., Cartinhour, S., Chatterjee, A.K., D'Ascenzo, M., Gwinn, M.L., Lazarowitz, S.G., et al. (2002). Genomewide identification of Pseudomonas syringae pv. tomato DC3000 promoters controlled by the HrpL alternative sigma factor. Proc. Natl. Acad. Sci. USA *99*, 2275–2280.

Friedrich, L., Vernooij, B., Gaffney, T., Morse, A., and Ryals, J. (1995). Characterization of tobacco plants expressing a bacterial salicylate hydroxylase gene. Plant Mol. Biol. *29*, 959–968.

Fry, W.E., Birch, P.R., Judelson, H.S., Grünwald, N.J., Danies, G., Everts, K.L., Gevens, A.J., Gugino, B.K., Johnson, D.A., Johnson, S.B., et al. (2015). Five Reasons to Consider Phytophthora infestans a Reemerging Pathogen. Phytopathology *105*, 966–981.

Gassmann, W., and Bhattacharjee, S. (2012). Effector-triggered immunity signaling: from gene-for-gene pathways to protein-protein interaction networks. Mol. Plant Microbe Interact. *25*, 862–868.

Glazebrook, J. (2005). Contrasting mechanisms of defense against biotrophic and necrotrophic pathogens. Annu. Rev. Phytopathol. *43*, 205–227.

Glick, B.R. (2012). Plant growth-promoting bacteria: mechanisms and applications. Scientifica (Cairo) *2012*, 963401.

Gopalan, S., Bauer, D.W., Alfano, J.R., Loniello, A.O., He, S.Y., and Collmer, A. (1996). Expression of the Pseudomonas syringae avirulence protein AvrB in plant cells alleviates its dependence on the hypersensitive response and pathogenicity (Hrp) secretion system in eliciting genotype-specific hypersensitive cell death. Plant Cell *8*, 1095–1105.

Guo, M., Tian, F., Wamboldt, Y., and Alfano, J.R. (2009). The majority of the type III effector inventory of Pseudomonas syringae pv. tomato DC3000 can suppress plant immunity. Mol. Plant Microbe Interact. *22*, 1069–1080.

Haas, D., and Défago, G. (2005). Biological control of soil-borne pathogens by fluorescent pseudomonads. Nat. Rev. Microbiol. *3*, 307–319.

Hammoudi, V., Fokkens, L., Beerens, B., Vlachakis, G., Chatterjee, S., Arroyo-Mateos, M., Wackers, P.F.K., Jonker, M.J., and van den Burg, H.A. (2018). The Arabidopsis SUMO E3 ligase SIZ1 mediates the temperature dependent trade-off between plant immunity and growth. PLoS Genet. *14*, e1007157.

Horspool, A.M., and Schertzer, J.W. (2018). Reciprocal cross-species induction of outer membrane vesicle biogenesis via secreted factors. Sci. Rep. *8*, 9873.

Horstman, A.L., and Kuehn, M.J. (2000). Enterotoxigenic Escherichia coli secretes active heat-labile enterotoxin via outer membrane vesicles. J. Biol. Chem. *275*, 12489–12496.

Huot, B., Yao, J., Montgomery, B.L., and He, S.Y. (2014). Growth-defense tradeoffs in plants: a balancing act to optimize fitness. Mol. Plant *7*, 1267–1287.

Iavicoli, A., Boutet, E., Buchala, A., and Métraux, J.-P. (2003). Induced systemic resistance in Arabidopsis thaliana in response to root inoculation with Pseudomonas fluorescens CHA0. Mol. Plant Microbe Interact. *16*, 851–858.

Ionescu, M., Zaini, P.A., Baccari, C., Tran, S., da Silva, A.M., and Lindow, S.E. (2014). Xylella fastidiosa outer membrane vesicles modulate plant colonization by blocking attachment to surfaces. Proc. Natl. Acad. Sci. USA *111*, E3910–E3918.

Jones, J.D., and Dangl, J.L. (2006). The plant immune system. Nature *444*, 323–329.

Jung, H.W., Tschaplinski, T.J., Wang, L., Glazebrook, J., and Greenberg, J.T. (2009). Priming in systemic plant immunity. Science *324*, 89–91.

Kamoun, S., Furzer, O., Jones, J.D., Judelson, H.S., Ali, G.S., Dalio, R.J., Roy, S.G., Schena, L., Zambounis, A., Panabières, F., et al. (2015). The Top 10 oomycete pathogens in molecular plant pathology. Mol. Plant Pathol. *16*, 413–434.

Kaparakis-Liaskos, M., and Ferrero, R.L. (2015). Immune modulation by bacterial outer membrane vesicles. Nat. Rev. Immunol. *15*, 375–387.

Katagiri, F., Thilmony, R., and He, S.Y. (2002). The Arabidopsis thaliana-pseudomonas syringae interaction. Arabidopsis Book *1*, e0039.

Keenan, J.I., and Allardyce, R.A. (2000). Iron influences the expression of *Helicobacter pylori* outer membrane vesicle-associated virulence factors. Eur. J. Gastroenterol. Hepatol. *12*, 1267–1273.

Kesty, N.C., Mason, K.M., Reedy, M., Miller, S.E., and Kuehn, M.J. (2004). Enterotoxigenic Escherichia coli vesicles target toxin delivery into mammalian cells. EMBO J. *23*, 4538–4549.

Kuehn, M.J., and Kesty, N.C. (2005). Bacterial outer membrane vesicles and the host-pathogen interaction. Genes Dev. *19*, 2645–2655.

Kulkarni, H.M., and Jagannadham, M.V. (2014). Biogenesis and multifaceted roles of outer membrane vesicles from Gram-negative bacteria. Microbiology (Reading) *160*, 2109–2121.

Kulkarni, H.M., Swamy, ChV., and Jagannadham, M.V. (2014). Molecular characterization and functional analysis of outer membrane vesicles from the antarctic bacterium Pseudomonas syringae suggest a possible response to environmental conditions. J. Proteome Res. *13*, 1345–1358.

Kulkarni, H.M., Swamy, ChV., and Jagannadham, M.V. (2015). The proteome of the outer membrane vesicles of an Antarctic bacterium Pseudomonas syringae Lz4W. Data Brief *4*, 406–409.

Kulp, A., and Kuehn, M.J. (2010). Biological functions and biogenesis of secreted bacterial outer membrane vesicles. Annu. Rev. Microbiol. *64*, 163–184.

Kulp, A.J., Sun, B., Ai, T., Manning, A.J., Orench-Rivera, N., Schmid, A.K., and Kuehn, M.J. (2015). Genome-Wide Assessment of Outer Membrane Vesicle Production in Escherichia coli. PLoS ONE *10*, e0139200.

Lam, H.N., Chakravarthy, S., Wei, H.L., BuiNguyen, H., Stodghill, P.V., Collmer, A., Swingle, B.M., and Cartinhour, S.W. (2014). Global analysis of the HrpL regulon in the plant pathogen Pseudomonas syringae pv. tomato DC3000 reveals new regulon members with diverse functions. PLoS ONE *9*, e106115.

Lawton, K.A., Friedrich, L., Hunt, M., Weymann, K., Delaney, T., Kessmann, H., Staub, T., and Ryals, J. (1996). Benzothiadiazole induces disease resistance in Arabidopsis by activation of the systemic acquired resistance signal transduction pathway. Plant J. *10*, 71–82.

Lindgren, P.B., Peet, R.C., and Panopoulos, N.J. (1986). Gene cluster of Pseudomonas syringae pv. "phaseolicola" controls pathogenicity of bean plants and hypersensitivity of nonhost plants. J. Bacteriol. *168*, 512–522.

Liu, L., Sonbol, F.-M., Huot, B., Gu, Y., Withers, J., Mwimba, M., Yao, J., He, S.Y., and Dong, X. (2016). Salicylic acid receptors activate jasmonic acid signalling through a non-canonical pathway to promote effector-triggered immunity. Nat. Commun. *7*, 13099.

Lomovatskaya, L.A., and Romanenko, A.S. (2020). Secretion Systems of Bacterial Phytopathogens and Mutualists. Appl. Biochem. Microbiol. *56*, 115–129.

Loper, J.E., Kobayashi, D.Y., and Paulsen, I.T. (2007). The Genomic Sequence of Pseudomonas fluorescens Pf-5: Insights Into Biological Control. Phytopathology *97*, 233–238.

Lozano-Durán, R., and Zipfel, C. (2015). Trade-off between growth and immunity: role of brassinosteroids. Trends Plant Sci. *20*, 12–19.

Manning, A.J., and Kuehn, M.J. (2011). Contribution of bacterial outer membrane vesicles to innate bacterial defense. BMC Microbiol. *11*, 258.

Maurhofer, M., Hase, C., Meuwly, P., Metraux, J.P., and Defago, G. (1994). Induction of systemic resistance of tobacco to tobacco necrosis virus by the root-colonizing Pseudomonas fluorescens strain CHA0: influence of the gacA gene and of pyoverdine production. Phytopathology *84*, 139–146.

Mazurier, S., Merieau, A., Bergeau, D., Decoin, V., Sperandio, D., Crépin, A., Barbey, C., Jeannot, K., Vicré-Gibouin, M., Plésiat, P., et al. (2015). Type III secretion system and virulence markers highlight similarities and differences between human- and plant-associated pseudomonads related to Pseudomonas fluorescens and P. putida. Appl. Environ. Microbiol. *81*, 2579–2590.

McBroom, A.J., and Kuehn, M.J. (2007). Release of outer membrane vesicles by Gram-negative bacteria is a novel envelope stress response. Mol. Microbiol. *63*, 545–558.

McBroom, A.J., Johnson, A.P., Vemulapalli, S., and Kuehn, M.J. (2006). Outer membrane vesicle production by Escherichia coli is independent of membrane instability. J. Bacteriol. *188*, 5385–5392.

Mcdowell, J.M. (2014). Hyaloperonospora arabidopsidis: A Model Pathogen of Arabidopsis. In Genomics of Plant-Associated Fungi and Oomycetes: Dicot Pathogens, R.A. Dean, A. Lichens-Park, and C. Kole, eds. (Springer).

Morgunov, I.G., Kamzolova, S.V., Dedyukhina, E.G., Chistyakova, T.I., Lunina, J.N., Mironov, A.A., Stepanova, N.N., Shemshura, O.N., and Vainshtein, M.B. (2017). Application of organic acids for plant protection against phytopathogens. Appl. Microbiol. Biotechnol. *101*, 921–932.

Navarro, L., Bari, R., Achard, P., Lisón, P., Nemri, A., Harberd, N.P., and Jones, J.D.G. (2008). DELLAs control plant immune responses by modulating the balance of jasmonic acid and salicylic acid signaling. Curr. Biol. *18*, 650–655.

Nomura, H., Komori, T., Uemura, S., Kanda, Y., Shimotani, K., Nakai, K., Furuichi, T., Takebayashi, K., Sugimoto, T., Sano, S., et al. (2012). Chloroplast-mediated activation of plant immune signalling in Arabidopsis. Nat. Commun. *3*, 926.

Orench-Rivera, N., and Kuehn, M.J. (2016). Environmentally controlled bacterial vesicle-mediated export. Cell. Microbiol. *18*, 1525–1536.

Park, S.W., Liu, P.P., Forouhar, F., Vlot, A.C., Tong, L., Tietjen, K., and Klessig, D.F. (2009). Use of a synthetic salicylic acid analog to investigate the roles of methyl salicylate and its esterases in plant disease resistance. J. Biol. Chem. *284*, 7307–7317.

Pathirana, R.D., and Kaparakis-Liaskos, M. (2016). Bacterial membrane vesicles: biogenesis, immune regulation and pathogenesis. Cell. Microbiol. *18*, 1518–1524.

Paulsson, M., Che, K.F., Ahl, J., Tham, J., Sandblad, L., Smith, M.E., Qvarfordt, I., Su, Y.C., Lindén, A., and Riesbeck, K. (2018). Bacterial Outer Membrane Vesicles Induce Vitronectin Release Into the Bronchoalveolar Space Conferring Protection From Complement-Mediated Killing. Front. Microbiol. *9*, 1559.

Pieterse, C.M.J., Zamioudis, C., Berendsen, R.L., Weller, D.M., Van Wees, S.C., and Bakker, P.A. (2014). Induced systemic resistance by beneficial microbes. Annu. Rev. Phytopathol. *52*, 347–375.

Pirhonen, M.U., Lidell, M.C., Rowley, D.L., Lee, S.W., Jin, S., Liang, Y., Silverstone, S., Keen, N.T., and Hutcheson, S.W. (1996). Phenotypic expression of Pseudomonas syringae avr genes in E. coli is linked to the activities of the hrp-encoded secretion system. Mol. Plant Microbe Interact. *9*, 252–260.

Prados-Rosales, R., Weinrick, B.C., Piqué, D.G., Jacobs, W.R., Jr., Casadevall, A., and Rodriguez, G.M. (2014). Role for Mycobacterium tuberculosis membrane vesicles in iron acquisition. J. Bacteriol. *196*, 1250–1256.

Ranf, S. (2016). Immune Sensing of Lipopolysaccharide in Plants and Animals: Same but Different. PLoS Pathog. *12*, e1005596.

Ristaino, J., Cooke, D., Acuña, I., and Muñoz, M. (2019). The threat of late blight to global food security. Emerging Plant Disease and Global Food Security, A. Records and J. Ristaino, eds. (American Phytopathological Society Press).

Rodriguez, B.V., and Kuehn, M.J. (2020). Staphylococcus aureus secretes immunomodulatory RNA and DNA via membrane vesicles. Sci. Rep. *10*, 18293.

Roier, S., Zingl, F.G., Cakar, F., Durakovic, S., Kohl, P., Eichmann, T.O., Klug, L., Gadermaier, B., Weinzerl, K., Prassl, R., et al. (2016). A novel mechanism for the biogenesis of outer membrane vesicles in Gram-negative bacteria. Nat. Commun. *7*, 10515.

Roine, E., Wei, W., Yuan, J., Nurmiaho-Lassila, E.L., Kalkkinen, N., Romantschuk, M., and He, S.Y. (1997). Hrp pilus: an hrp-dependent bacterial surface appendage produced by Pseudomonas syringae pv. tomato DC3000. Proc. Natl. Acad. Sci. USA *94*, 3459–3464.

Santoyo, G., Orozco-Mosqueda, M.D.C., and Govindappa, M. (2012). Mechanisms of biocontrol and plant growth-promoting activity in soil bacterial species of Bacillus and Pseudomonas: a review. Biocontrol Sci. Technol. *22*, 855–872.

Schreiber, K., Ckurshumova, W., Peek, J., and Desveaux, D. (2008). A high-throughput chemical screen for resistance to Pseudomonas syringae in Arabidopsis. Plant J. *54*, 522–531.

Schwechheimer, C., and Kuehn, M.J. (2015). Outer-membrane vesicles from Gram-negative bacteria: biogenesis and functions. Nat. Rev. Microbiol. *13*, 605–619.

Schwechheimer, C., Sullivan, C.J., and Kuehn, M.J. (2013). Envelope control of outer membrane vesicle production in Gram-negative bacteria. Biochemistry *52*, 3031–3040.

Schwechheimer, C., Kulp, A., and Kuehn, M.J. (2014). Modulation of bacterial outer membrane vesicle production by envelope structure and content. BMC Microbiol. *14*, 324.

Schwechheimer, C., Rodriguez, D.L., and Kuehn, M.J. (2015). NlpI-mediated modulation of outer membrane vesicle production through peptidoglycan dynamics in Escherichia coli. MicrobiologyOpen *4*, 375–389.

Shah, J., and Zeier, J. (2013). Long-distance communication and signal amplification in systemic acquired resistance. Front. Plant Sci. *4*, 30.

Shen, H., and Keen, N.T. (1993). Characterization of the promoter of avirulence gene D from Pseudomonas syringae pv. tomato. J. Bacteriol. *175*, 5916–5924.

Sidhu, V.K., Vorhölter, F.J., Niehaus, K., and Watt, S.A. (2008). Analysis of outer membrane vesicle associated proteins isolated from the plant pathogenic bacterium Xanthomonas campestris pv. campestris. BMC Microbiol. *8*, 87.

Silipo, A., Erbs, G., Shinya, T., Dow, J.M., Parrilli, M., Lanzetta, R., Shibuya, N., Newman, M.-A., and Molinaro, A. (2010). Glyco-conjugates as elicitors or suppressors of plant innate immunity. Glycobiology *20*, 406–419.

Sivasakthi, S., Usharani, G., and Saranraj, P. (2014). Biocontrol potentiality of plant growth promoting bacteria (PGPR) - Pseudomonas fluorescens and Bacillus subtilis: a review. Afr. J. Agric. Res. *9*, 1265–1277.

Solé, M., Scheibner, F., Hoffmeister, A.K., Hartmann, N., Hause, G., Rother, A., Jordan, M., Lautier, M., Arlat, M., and Büttner, D. (2015). Xanthomonas campestris pv. vesicatoria Secretes Proteases and Xylanases via the Xps Type II Secretion System and Outer Membrane Vesicles. J. Bacteriol. *197*, 2879–2893.

Spoel, S.H., and Dong, X. (2012). How do plants achieve immunity? Defence without specialized immune cells. Nat. Rev. Immunol. *12*, 89–100.

Stael, S., Kmiecik, P., Willems, P., Van Der Kelen, K., Coll, N.S., Teige, M., and Van Breusegem, F. (2015). Plant innate immunity–sunny side up? Trends Plant Sci. *20*, 3–11.

Su, J., Yang, L., Zhu, Q., Wu, H., He, Y., Liu, Y., Xu, J., Jiang, D., and Zhang, S. (2018). Active photosynthetic inhibition mediated by MPK3/MPK6 is critical to effector-triggered immunity. PLoS Biol. *16*, e2004122.

Summermatter, K., Sticher, L., and Metraux, J.P. (1995). Systemic Responses in Arabidopsis thaliana Infected and Challenged with Pseudomonas syringae pv syringae. Plant Physiol. *108*, 1379–1385.

Suzuki, H., Nishimura, Y., Yasuda, S., Nishimura, A., Yamada, M., and Hirota, Y. (1978). Murein-lipoprotein of Escherichia coli: a protein involved in the stabilization of bacterial cell envelope. Mol. Gen. Genet. *167*, 1–9.

Tayi, L., Maku, R., Patel, H.K., and Sonti, R.V. (2016). Action of Multiple Cell Wall-Degrading Enzymes Is Required for Elicitation of Innate Immune Responses During Xanthomonas oryzae pv. oryzae Infection in Rice. Mol. Plant Microbe Interact. *29*, 599–608.

Tedman-Jones, J.D., Lei, R., Jay, F., Fabro, G., Li, X., Reiter, W.D., Brearley, C., and Jones, J.D.G. (2008). Characterization of Arabidopsis mur3 mutations that result in constitutive activation of defence in petioles, but not leaves. Plant J. *56*, 691–703.

Thilmony, R., Underwood, W., and He, S.Y. (2006). Genome-wide transcriptional analysis of the Arabidopsis thaliana interaction with the plant pathogen Pseudomonas syringae pv. tomato DC3000 and the human pathogen Escherichia coli O157:H7. Plant J. *46*, 34–53.

Tran, H., Ficke, A., Asiimwe, T., Höfte, M., and Raaijmakers, J.M. (2007). Role of the cyclic lipopeptide massetolide A in biological control of Phytophthora infestans and in colonization of tomato plants by Pseudomonas fluorescens. New Phytol. *175*, 731–742.

Tsuda, K., Sato, M., Glazebrook, J., Cohen, J.D., and Katagiri, F. (2008). Interplay between MAMP-triggered and SA-mediated defense responses. Plant J. *53*, 763–775.

Tsuda, K., Sato, M., Stoddard, T., Glazebrook, J., and Katagiri, F. (2009). Network properties of robust immunity in plants. PLoS Genet. *5*, e1000772.

Tsuda, K., Mine, A., Bethke, G., Igarashi, D., Botanga, C.J., Tsuda, Y., Glazebrook, J., Sato, M., and Katagiri, F. (2013). Dual regulation of gene expression mediated by extended MAPK activation and salicylic acid contributes to robust innate immunity in Arabidopsis thaliana. PLoS Genet. *9*, e1004015.

Volgers, C., Savelkoul, P.H.M., and Stassen, F.R.M. (2018). Gram-negative bacterial membrane vesicle release in response to the host-environment: different threats, same trick? Crit. Rev. Microbiol. *44*, 258–273.

Wang, D., Amornsiripanitch, N., and Dong, X. (2006). A genomic approach to identify regulatory nodes in the transcriptional network of systemic acquired resistance in plants. PLoS Pathog. *2*, e123.

Wang, W., Barnaby, J.Y., Tada, Y., Li, H., Tör, M., Caldelari, D., Lee, D.-U., Fu, X.-D., and Dong, X. (2011). Timing of plant immune responses by a central circadian regulator. Nature *470*, 110–114.

Wang, X., Thompson, C.D., Weidenmaier, C., and Lee, J.C. (2018). Release of Staphylococcus aureus extracellular vesicles and their application as a vaccine platform. Nat. Commun. *9*, 1379.

Weller, D.M., Mavrodi, D.V., van Pelt, J.A., Pieterse, C.M.J., van Loon, L.C., and Bakker, P.A.H.M. (2012). Induced systemic resistance in Arabidopsis thaliana against Pseudomonas syringae pv. tomato by 2,4-diacetylphloroglucinol-producing Pseudomonas fluorescens. Phytopathology *102*, 403–412.

Wildermuth, M.C., Dewdney, J., Wu, G., and Ausubel, F.M. (2001). Isochorismate synthase is required to synthesize salicylic acid for plant defence. Nature *414*, 562–565.

Xin, X.F., and He, S.Y. (2013). Pseudomonas syringae pv. tomato DC3000: a model pathogen for probing disease susceptibility and hormone signaling in plants. Annu. Rev. Phytopathol. *51*, 473–498.

Xin, X.-F., Nomura, K., Aung, K., Velásquez, A.C., Yao, J., Boutrot, F., Chang, J.H., Zipfel, C., and He, S.Y. (2016). Bacteria establish an aqueous living space in plants crucial for virulence. Nature *539*, 524–529.

Xu, G., Greene, G.H., Yoo, H., Liu, L., Marqués, J., Motley, J., and Dong, X. (2017). Global translational reprogramming is a fundamental layer of immune regulation in plants. Nature *545*, 487–490.

Yem, D.W., and Wu, H.C. (1978). Physiological characterization of an Escherichia coli mutant altered in the structure of murein lipoprotein. J. Bacteriol. *133*, 1419–1426.

Zamioudis, C., and Pieterse, C.M. (2012). Modulation of host immunity by beneficial microbes. Mol. Plant Microbe Interact. *25*, 139–150.

Zheng, X.-Y., Spivey, N.W., Zeng, W., Liu, P.P., Fu, Z.Q., Klessig, D.F., He, S.Y., and Dong, X. (2012). Coronatine promotes Pseudomonas syringae virulence in plants by activating a signaling cascade that inhibits salicylic acid accumulation. Cell Host Microbe *11*, 587–596.

Zhou, L., Srisatjaluk, R., Justus, D.E., and Doyle, R.J. (1998). On the origin of membrane vesicles in gram-negative bacteria. FEMS Microbiol. Lett. *163*, 223–228.

Zingl, F.G., Kohl, P., Cakar, F., Leitner, D.R., Mitterer, F., Bonnington, K.E., Rechberger, G.N., Kuehn, M.J., Guan, Z., Reidl, J., and Schild, S. (2020). Outer Membrane Vesiculation Facilitates Surface Exchange and In Vivo Adaptation of Vibrio cholerae. Cell Host Microbe *27*, 225–237.e8.

STAR★METHODS

KEY RESOURCES TABLE

REAGENT or RESOURCE	SOURCE	IDENTIFIER
Antibodies		
Phospho-p44/42 MAPK	Cell Signaling	CAT# 9101
Bacterial and virus strains		
Pseudomonas syringae pv *tomato* DC3000	Xinnian Dong, Duke University (MK lab stock #1334)	N/A
Pseudomonas fluorescens Migula	ATCC (MK lab stock #1335)	CAT# 13535
Pseudomonas aeruginosa S470	Meta J. Kuehn, DUMC Clinical Isolate (MK lab stock #222)	N/A
Enterotoxigenic *Escherichia coli* H10407	ATCC (MK lab stock #378)	CAT# 35401
Staphylococcus aureus Newman	Ken Yokoyama, Duke University (MK lab stock #1336)	N/A
Hyaloperonospora arabidopsidis NOCO2	Xinnian Dong, Duke University	N/A
Phytophthora infestans NC14-1 (Clonal Lineage US-23)	Jean B. Ristaino, North Carolina State University	N/A
Chemicals, peptides, and recombinant proteins		
Bradford Reagent	VWR	CAT# 97065-010
FM4-64	Thermo Fisher/ Invitrogen	CAT# T13320
OptiPrep Density Gradient Medium	Sigma	CAT# D1556
Sytox Green	Thermo Fisher/ Invitrogen	CAT# S7020
SuperSignal West Dura substrate	Thermo Fisher	CAT# 34075
Experimental models: organisms/strains		
Arabidopsis thaliana ecotype Columbia-0 (Col-0)	Xinnian Dong, Duke University	N/A
Arabidopsis thaliana ICS1-LUC	Xinnian Dong, Duke University (Tedman-Jones et al., 2008)	N/A
Arabidopsis thaliana dde2-2/ein2-1/pad4-1/sid2-2 (DEPS)	ABRC	Stock# CS66007
Arabidopsis thaliana dde2-2/ein2-1/pad4-1 (DEP)	ABRC	Stock# CS66004
Arabidopsis thaliana dde2-2/pad4-1/sid2-2 (DPS)	ABRC	Stock# CS66005
Arabidopsis thaliana ein2-1/pad4-1/sid2-2 (EPS)	ABRC	Stock# CS66006
Solanum lycopersicum cv Mountain Fresh Plus	Jean B. Ristaino, North Carolina State University	N/A
Software and algorithms		
FIJI	NIH	https://imagej.net/Fiji
JMP Pro14	SAS	https://www.jmp.com/en_us/software/data-analysis-software.html
Other		
MetroMix 360 Growing Medium	SunGro Horticulture	CAT# GP92031
Sunshine Redi-Earth Pro Growing Mix	SunGro Horticulture	CAT# GP92747

RESOURCE AVAILABILITY

Lead contact

Further information and requests for resources and reagents should be directed to and will be fulfilled by the Lead Contact, Meta J. Kuehn (kuehn@duke.edu).

Materials availability

This study did not generate new unique reagents.

Data and code availability

The published article includes all datasets generated and analyzed during this study.

EXPERIMENTAL MODEL AND SUBJECT DETAILS

Bacterial strains and culture conditions

Pseudomonas syringae pv *tomato* DC3000 was inoculated from frozen glycerol stocks onto King's Broth (KB) agar plates [2% proteose peptone, 8.6 mM K_2HPO_4, 1.4% glycerol, 6 mM $MgSO_4$, 1.5% agar] supplemented with 25 mg/mL [30.4 mM] Rifampicin and grown for two days at 28°C. Colonies were used to inoculate 50 mL liquid KB media supplemented with Rifampicin and incubated overnight at 28°C with constant shaking. Aliquots of this overnight culture (1 mL) were used to inoculate 0.5-1 L cultures of KB with Rifampicin, which were incubated at 28°C with constant shaking for 17 h to reach early stationary phase. Shaking speed was reduced to 150 rpm to reduce foam accumulation. To shift to minimal media, cells were pelleted in a Beckman Avanti J-25 centrifuge (JLA-10.500 rotor; 10,000 x g; 10 min), supernatant was discarded, and cell pellets were resuspended in minimal media and incubated for 2 h at 28°C. Minimal media consisted of minimal salts [20.2 mM KH_2PO_4, 4.3 mM K_2HPO_4, 3.8 mM $(NH_4)_2SO_4$, 0.85 mM $MgCl_2$, 0.86 mM NaCl, pH to 5 using HCl] supplemented with 0.01% [0.56 mM] fructose. *Pseudomonas fluorescens* Migula ATCC 13525 was cultured as above without Rifampicin. Culturing of other bacterial species was as described previously (*P. aeruginosa*, (Esoda and Kuehn, 2019), Enterotoxigenic *E. coli*, (Manning and Kuehn, 2011), *S. aureus*, (Wang et al., 2018).

Oomycete strains and propagation conditions

For propagation, 10-day-old *A. thaliana* seedlings were sprayed with 3-5 × 10^4 spores of *Hyaloperonospora arabidopsidis* NOCO2 isolate. Plants were covered with a plastic dome and placed in 12 h light/12 h dark growth incubator. Plants were then covered with a mesh dome and returned to the growth incubator for 6 days. Sporangiophores were collected by placing sporulating plants in 30 mL of water and vortexing. Plants were removed and the suspension was used to inoculate seedlings.

P. infestans isolate NC 14-1 (clonal lineage US-23) was grown and maintained on detached leaves of *Solanum lycopersicum* cv. Mountain Fresh Plus under 1.5% water agar in ambient laboratory conditions for seven days prior to inoculation. Sporangia were harvested from these leaves by placing the infected leaf in a 15 mL tube with 10 mL dH_2O and shaking vigorously to release sporangia.

Plant lines and growth conditions

Seeds from *Arabidopsis thaliana* were either sown on autoclaved soil (MetroMix 360, SunGro Horticulture) with added fertilizer and vernalized (2 days; 4°C in the dark) before transferring to 16 h of light/8 h of dark at 28°C, or sterilized using isopropyl alcohol and bleach solution, vernalized (4°C; shaking in dH_2O; 2 days), and grown vertically on Murashige and Skoog (MS) agar plates [2.3 mM MES, 0.43% MS Basal Salts (Caisson Labs, macro- and micronutrients), pH 5.7 with 1 M KOH, 58.4 mM sucrose, 0.1% MS Vitamins (Caisson Labs), 0.4% agar), at room temperature under 16 h of light/8 h of dark. Further details are provided in the method details.

This study used *A. thaliana* ecotype Columbia-0 (Col-0) as the wild-type, as well as seeds from transgenic *A. thaliana* plants encoding a luciferase reporter fused to the *ICS1* promoter in the Col-0 background (*ICS1*:LUC) previously described (Tedman-Jones et al., 2008), and several *A. thaliana* hormone mutants available through the *Arabidopsis* Biological Resource Center (ABRC). These mutants were *dde2-2/ein2-1/pad4-1/sid2-2* (DEPS, Stock Number CS66007); *dde2-2/ein2-1/pad4-1* (DEP, Stock Number CS66004); *dde2-2/pad4-1/sid2-2* (DPS, Stock Number CS66005); *ein2-1/pad4-1/sid2-2* (EPS, Stock Number CS66006).

Solanum lycopersicum cv. Mountain Fresh Plus seedlings were grown from seed in potting mix (50% Sunshine Redi-Earth Pro Growing Mix [50 – 65% Canadian Sphagnum peat moss, vermiculite, dolomitic lime, 0.0001% Silicon dioxide], 50% cement sand) and cultivated in a Phytotron greenhouse under 14 h of light per day (natural light supplemented with artificial light) with a 26°C / 22°C day / night temperature cycle. Leaves were collected from four-to-six-week-old tomato plants at the five-to-six leaf stage and used for all experiments.

METHOD DETAILS

Bacterial OMV/MV preparations

OMVs were purified according to published protocols with a few modifications (Bauman and Kuehn, 2006). Cells were pelleted from cultures in a Beckman Avanti J-25 centrifuge (JLA-10.500 rotor; 10,000 x g; 10 min), supernatant was collected and filtered (0.45 μm

HV, Millipore Durapore) to remove any contaminating bacterial cells. OMVs were then concentrated using tangential flow (Cole-Parmer MasterFlex) with a 100 kDa cutoff filter (Pall Corporation). OMV concentrate was filtered again (0.45 μm HV, Millipore). OMVs were pelleted from the concentrate in a Beckman Avanti J-25 centrifuge (JLA-16.250 rotor; 35,000 x g; 3 h), and resuspended in 1 mL minimal media for 1 h at 4°C. OMVs were filtered for sterilization (0.45 μm HV, Millipore Durapore), before pelleting in a Beckman Optima TLX ultracentrifuge (TLA-100.3 rotor; 90,935 x g (max); 1 h). The OMV pellet was resuspended in 100 μL minimal media (overnight; 4°C) before protein and lipid quantitation. OMVs were used for experimentation within the week or stored at −20°C. *Sa* MVs were purified according to Rodriguez and Kuehn (2020).

For the Bradford assay, concentrated OMVs/MVs were diluted 4 times in dH_2O and 5 μL of this dilution was added to 150 μL Bradford reagent (VWR). Absorbance was measured at 595 nm and compared to a standard curve to calculate protein concentration. Each sample was measured in duplicate. For the FM4-64 assay, concentrated OMVs/MVs were diluted 4 times in dH_2O to a final volume of 20 μL. Diluted OMVs/MVs were added to 560 μL of DPBSS buffer [2.7 mM KCl, 1.5 mM KH_2PO_4, 200.2 mM NaCl; 4.3 mM Na_2HPO_4, 0.5 mM $MgCl_2 \cdot 6H_2O$, 0.7 mM $CaCl_2$] and 20 μL of FM4-64 (100 ng/mL; Invitrogen) and incubated in the dark (37°C; 10 min; shaking). A negative control was prepared by adding 580 μL of DPBSS buffer to 20 μL of FM4-64 (100 ng/mL; Invitrogen) and incubated as the OMV/MV samples. 260 μL of each sample was added in duplicate to a 96-well black clear bottom plate and fluorescence measured in a plate reader (506 nm excitation, 750 nm emission; Molecular Devices SpectraMax). Background due to media was subtracted.

For density gradient purification of OMVs, 1.5 mL 60% Optiprep (Sigma) in dH_2O was mixed with 0.5 mL of the pelleted OMV-containing preparation and loaded on top of a 1 mL cushion of 60% Optiprep/dH_2O at the bottom of a 12.5 mL ultracentrifuge tube. These were followed by layers (2 mL each) of 40%, 35%, 30%, 25%, and (1 mL) 20% Optiprep/dH_2O. Gradients were centrifuged in a Beckman Optima LE-80K ultracentrifuge (SW 41 Ti rotor; 27,500 x g; 12-14 h; 4°C). Fractions (1 mL) were collected from the top of the gradient. For reference, the fractions resulting from an empty gradient of the same proportions from lightest (top) to heaviest (bottom) were measured in triplicate using a portable refractometer (Fisher Scientific; Brix 28%–62%). Their mean densities were < 28%, < 28%, < 28%, 28%, 30.5%, 32.7%, 34.7%, 36.8%, 40.2%, 43.7%, 46.2%, and 58.3%. Optiprep/dH_2O was removed by washing two times in 25 mL sterile, dH_2O in a Beckman Optima LE-80K ultracentrifuge (50.2 Ti rotor; 41,000 x g; 1 hr; 4°C). Pellets were resuspended in 1 mL sterile, dH_2O, analyzed using Bradford, FM4-64, and TEM, and used in bacterial challenge and seedling growth inhibition experiments.

OMV/MV concentration for use in experiments was calculated based on the amount needed for *ICS1* expression assays (see below). For these assays, plants were treated with equal amounts of protein from bacterial cell suspensions (standard concentration of bacterial cells at OD_{600} 0.02 in 10 mM Mg_2SO_4) and OMV/MV preparations. To calculate an equivalent concentration of OMVs/MVs to add, protein was measured in the bacterial suspension at the concentration used. *Pst* cells from minimal media at OD_{600} 0.02 contained 2.74 μg/mL of protein by Bradford assay. We used this concentration as our "1X" concentration of OMVs/MVs throughout all experiments for all bacterial species tested. Five times this amount, 13.7 μg/mL of protein, was used as the "5X" concentration for OMVs/MVs throughout all experiments for all bacterial species tested. Based on calculations from the yield table (Table S1), *Pst* cells in minimal media at OD_{600} 0.02 produce approximately 9.1 μg/mL of OMVs based on protein. Therefore, the 5X concentration is approximately 1.5X the concentration of OMVs that would be produced by a standard *Pst* inoculum used in bacterial challenge assays (Zheng et al., 2012; Schreiber et al., 2008).

Sytox Green assay

Membrane integrity was assessed as previously published (Bonnington and Kuehn, 2016). Five samples were prepared for the Sytox Green assay to measure membrane disruption. Two negative controls were prepared by adding 190 μL of KB or minimal media to 10 μL of Sytox Green (0.1 mM; Invitrogen). A positive control was prepared by taking a 200 μL aliquot of cells from a 1L culture grown in KB media, pelleting the cells in a Labnet Prism microcentrifuge (10,000 x g; 10 min), discarding 100 μL of the supernatant, and heating the remaining cell suspension in 10% SDS (100°C; 1 h). To this, 10 μL of Sytox Green (0.1 mM; Invitrogen) was added. Two experimental samples were prepared by taking 190 μL from a bacterial culture grown in KB media or shifted to minimal media and adding 10 μL of Sytox Green (0.1 mM; Invitrogen). In all samples, Sytox Green was added in the dark. All five samples were added to a 96-well black clear bottom plate, incubated (10 min; 37°C; shaking in the dark), and fluorescence measured in a plate reader (500 nm excitation, 550 nm emission; Molecular Devices SpectraMax).

TEM and negative staining

As previously published with some modifications (Manning and Kuehn, 2011), to prepare samples for TEM imaging, metal grids (Electron Microscopy Sciences; 300 mesh copper, formvar/carbon) were cleaned using the Pelco EasiGlow Machine Vacuum and then 10 μL of sample was added. Samples were pipetted onto the grid and let set for 1 min before wicking away excess with a Whatman filter paper. The samples were stained by applying 10 μL of 2% uranyl acetate, incubated 1.5 min, and excess uranyl acetate removed by wicking with Whatman filter paper. Grids were stored in Petri dishes at room temperature. Samples were imaged using a FEI Tecnai G^2 Twin Transmission Electron Microscope with a spot size of 2 at a voltage of 120kV.

ICS1 expression

As previously published (Tedman-Jones et al., 2008), seeds from transgenic plants encoding a luciferase reporter fused to the *ICS1* promoter were sown on autoclaved soil with added fertilizer and vernalized for 2 days at 4°C in the dark before transferring to 16 hours

of light/8 hours of dark at 28°C. After three weeks, two leaves per plant (leaves 3 and 4) were infiltrated with either bacterial cells at OD_{600} 0.02 or OMVs/MVs between 10 and 10:30 AM and plants were sprayed with luciferin substrate (1 mM). *ICS1* expression was then monitored over time by measuring luminescence in a gel doc (BioRad ChemiDoc XRS+).

SA/SAG extraction and quantification

SA/SAG was extracted and measured essentially as described (Liu et al., 2016; Zheng et al., 2012). To measure metabolite production, about 200 mg of leaf tissue was collected per replicate for each treatment condition and the precise weight recorded. Tissue was collected 52 h post treatment infiltration. Tissue was frozen in liquid nitrogen and ground to a powder with a metal bead in a GenoGrinder (500 strokes/min; SPEX Sample Prep). 600 μL of 90% methanol was added to each sample and vortexed. Samples were then sonicated for 16 min in an ice bath. Next, samples were centrifuged in an Eppendorf 5430 R centrifuge (FA-45-30-11 rotor; 20,800 x g; 5 min) and supernatant was collected and set aside. 600 μL of 100% methanol was added to the samples, vortexed, and sonicated for 16 min in an ice bath for a second time. Samples were centrifuged in an Eppendorf 5430 R centrifuge (FA-45-30-11 rotor; 20,800 x g; 5 min) and supernatant was combined with the supernatant from the initial extraction. Combined supernatant was centrifuged in an Eppendorf 5430 R centrifuge (FA-45-30-11 rotor; 20,800 x g; 5 min) to remove remaining debris. Supernatant from this spin was added to 50 μL of 0.2M NaOH and dried in a Speed-Vac (3 h; 20°C) covered with aluminum foil to avoid prolonged exposure to light. Dried residue was resuspended in 500 μL of 5% trichloracetic acid and sonicated for 16 min in an ice bath. Samples were centrifuged (20,800 x g; 5 min) and supernatant was collected.

Plants produce two forms of SA: the sugar-conjugated form, salicylic acid-2-O-β-D-glucoside (SAG), is produced for storage, and the unbound, free SA is thought to be liberated during an infection for use throughout the plant (Dempsey and Klessig, 2017; Summermatter et al., 1995; Blanco et al., 2009). Free SA is considered to be the biologically active form of the hormone (Park et al., 2009; Chaturvedi et al., 2012; Shah and Zeier, 2013; Spoel and Dong, 2012; Dempsey and Klessig, 2012).

Free SA was extracted 2 times with 500 μL of 1:1 ethyl acetate:cyclopentane, vortexed, sonicated in an ice bath for 16 minutes, and centrifuged (20,800 x g; 1 min) each time. The upper, aqueous phase was collected from both extractions, combined with 60 μL of High Pressure Liquid Chromatography (HPLC) eluent [10% methanol in 0.2% acetate buffer: 0.17% acetic acid, 56.0 mM NaAc, pH 5.5] and dried in a foil-covered Speed-Vac (45 min; 20°C). Samples were dried until 60 μL remained, diluted to 150 μL with HPLC eluent, and analyzed using HPLC with a C18 column (Agilent ZORBAX Eclipse XDB-C18).

Bound salicylic acid (SAG) was extracted by adding 20 μL of 12 N HCl to the combined organic phases of the extraction for free SA. Samples were heated (80°C; 1 h) and allowed to cool to room temperature slowly. Samples were then centrifuged (20,800 x g; 5 min) and the supernatant was collected. SAG was extracted 2 times with 500 μL 1:1 ethyl acetate:cyclopentane, vortexed, sonicated in an ice bath for 16 min, and centrifuged (20,800 x g; 1 min) each time. The organic phase from both extractions was combined, 60 μL of HPLC eluent was added, and the samples were dried at room temperature in a covered Speed-Vac. Samples were dried until 60 μL remained and then combined with 150 μL of HPLC eluent for HPLC analysis.

Experimental samples were compared to a negative control containing methanol and a standard curve established using dilutions of purified SA at 0.025, 0.05, 0.1, 0.2, 0.4, 1, 2, 4, and 20 ng/μL. SA was quantified by integrating the peaks from a spectrofluorometer (295-305 nm excitation/405-407 nm emission).

Seedling growth inhibition

As previously published with some modifications (Xu et al., 2017), seeds were sterilized using isopropyl alcohol and bleach solution prior to plating, and growth inhibition was measured as previously published with some modifications (Navarro et al., 2008). Briefly, seeds were shaken in isopropyl alcohol (70%; 10 min), rinsed with dH_2O, shaken in bleach (10%; 10 min), rinsed with dH_2O two times, shaken in dH_2O (10 min), then vernalized (4°C; shaking in dH_2O; 2 days). Seedlings were grown vertically on Murashige and Skoog (MS) agar plates [2.3 mM MES, 0.43% MS Basal Salts (Caisson Labs, macro- and micronutrients), pH 5.7 with 1 M KOH, 58.4 mM sucrose, 0.1% MS Vitamins (Caisson Labs), 0.4% agar), at room temperature under 16 h of light/8 h of dark. After 5 days, seedlings were transferred to liquid MS media in 96-well clear plates under sterile conditions. Plates were sealed with micropore tape and seedlings were returned to normal growth conditions. After 2 days, seedlings were treated with 10 mM Mg_2SO_4 or dH_2O buffer control or varying concentrations of OMVs/MVs. After 7 days, seedlings were removed from liquid media, blotted on a lint-free tissue to remove excess media, and weighed. For each experiment, 7 plants were grown per treatment. Each experiment was repeated 3 times.

Bacterial challenge

As described previously with some modifications (Wang et al., 2006), seeds were sown on autoclaved soil with added fertilizer and vernalized (2 days; 4°C in the dark) before transferring to 16 h of light/8 h of dark at 28°C. After three weeks, two leaves per plant (leaves 3 and 4) were infiltrated with OMVs/MVs between 10 and 10:30 AM and returned to the growth room overnight. 24 h later, leaves pre-treated with OMVs/MVs were infiltrated with *Pst*. *Pst* was grown for 2 days on KB agar plates at 28°C and suspended in 10 mM Mg_2SO_4 to an OD_{600} of 0.002 before infiltration. Plants were returned to the growth room for 4 days when leaf yellowing started to occur. Using a standard hole punch, discs were taken from each treated leaf and discs from the same plant were ground using a metal bead in 10 mM Mg_2SO_4. Samples were then serially diluted and plated in 10 μL strips on KB agar plates. Plates were incubated (2 d; 28°C) and then colony forming units were counted as a measure of bacterial growth.

OMV disruption

OMVs were isolated from minimal media as above and then exposed to a variety of disrupting conditions. Separately or in combination, OMVs were treated with polymyxin B sulfate (Sigma-Aldrich) (10 μM; 1 h; 37°C), sonication (30 min; in a water bath), Benzonase (Sigma ≥ 250 units/μL; 20%; 1 h; 37°C), Proteinase K (Sigma-Aldrich, 100 μg/mL; 1 h; 37°C), Tween 20 (2%; 10 min; 25°C), or boiling (100°C; 2 h). All OMV preparations were diluted to the 5X concentration (13.7 μg/mL protein) after the disruptions prior to plant infiltration to dilute potentially harmful concentrations of detergent. After diluting for infiltrations, samples contained 0.05% Tween 20. Salt-stripping was performed by treating OMVs with NaCl (2 M; 1 h; 25°C), pelleting in a Beckman Optima TLX ultracentrifuge (TLA-100.3 rotor; 90,935 x g (max); 1 h), separating the supernatant, and resuspending the stripped OMVs in dH_2O. For lyophilization, OMVs were flash-frozen in liquid nitrogen and then lyophilized for 1 h. For UV treatment, OMVs were exposed to 254 nm ultraviolet light (30 W) for 30 min.

MAPK activation

As previously published with some modifications (Xu et al., 2017). Phospho-p44/42 MAPK antibody (Cell Signaling #9101) was used at 1:4000 in 5% milk and exposed with SuperSignal West Dura substrate (Thermo Fisher).

H. arabidopsidis challenge

As described previously with some modifications (Wang et al., 2011), 3 pots per treatment of approximately 50 7-day old Col-0 *A. thaliana* seedlings were dipped into 10 mM $MgCl_2$ + 0.05% Silwet L77 or 5X OMVs in 10 mM $MgCl_2$ + 0.05% Silwet L77. Gentle vacuum was applied for 3 minutes and released slowly to infiltrate. Plants were covered with a plastic dome and placed in 12 h light/12 h dark growth incubator. 24 h post infiltration, plants were sprayed with 3-5 × 10^4 fresh spores of *Hyaloperonospora arabidopsidis* NOCO2 isolate. Plants were then covered with a mesh dome and returned to growth incubator for 6 days. On the 6th day post infection, plants were covered with a dome and watered heavily to increase humidity, then 10 plants were collected into 1 mL of dH_20 for three replicates per pot and vortexed to release spores. Spore density for each replicate was counted 3 times using a hemacytometer. Values are $x10^4$ unless otherwise noted.

P. infestans challenge

Vesicles were purified from *Pseudomonas syringae* pv tomato DC3000 and *Pseudomonas fluorescens* Migula ATCC 13525 and quantified by total protein (Bradford) and relative lipid amount (lipophilic dye FM4-64). Vesicles were diluted in 5 mL of buffer [10 mM MgCl2 + 0.05% Silwet L77] to a concentration of 27.4 μg/mL. Detached leaves of susceptible *Solanum lycopersicum* cv. Mountain Fresh Plus were dipped in either the buffer solution, *Pst* vesicles, or *Pf* vesicles and placed in a Petri dish abaxial side up. To infiltrate, a gentle vacuum (25 inHg) was applied for 5 min and released slowly. Leaves were allowed to dry for 6 h at room temperature before transferring under 1.5% water agar plates. Leaves were stored at room temperature under 12 h light/12 h dark for one day prior to late blight inoculation.

P. infestans isolate NC 14-1 (clonal lineage US-23) was grown and maintained on detached leaves of *Solanum lycopersicum* cv. Mountain Fresh Plus under 1.5% water agar in ambient laboratory conditions for seven days prior to inoculation. Sporangia were harvested from these leaves by placing the infected leaf in a 15 mL tube with 10 mL dH_2O and shaking vigorously to release sporangia. Sporangia were quantified using a hemocytometer and sporangial density was adjusted to 1000 sporangia/mL. 500 μL of this solution (500 sporangia) was misted onto the abaxial side of each inoculated leaf using a mist applicator attached to a 15 mL conical centrifuge tube. Conversely, 500 μL of diH_2O was misted onto the abaxial side of each uninoculated leaf. Leaves were then placed under 1.5% water agar in individual Petri plates, wrapped in parafilm, and incubated in plastic bins in ambient laboratory conditions under 12 h light/12 h dark. Sporangia concentration was measured 1-week post-inoculation. Sporangia for each leaf were harvested as above, and the number of sporangia/mL was quantified using a hemocytometer.

OMV organic extraction

Organic extractions were modified from previously published Lipid A preparations (Bonnington and Kuehn, 2016). Using protein to normalize starting amounts, 400 μg/mL of OMVs were diluted to 1 mL in HEPES buffer [50 mM HEPES free acid; pH to 7.4 with 10 mM NaOH] and added to a 12 mL glass vial. 4 mL of 2:1 methanol:dichloromethane was added to the vial, vortexed, and incubated at room temperature for 1 h. Samples were centrifuged in a Sorvall RC 6 Plus centrifuge (SH-3000 rotor; 828.4 x g; 30 min) and the supernatant was collected and set aside. This fraction contained the phospholipids. Pellets were washed with 5 mL of 2:1 methanol:dichloromethane and vortexed to resuspend. Samples were centrifuged in a Sorvall RC 6 Plus centrifuge (SH-3000 rotor; 828.4 x g; 20 min). Supernatant was collected and combined with the supernatant from the first extraction. Pellets were dried with nitrogen and resuspended in 150 μL dH_2O for use in the seedling growth inhibition assay or 350 μL dH_2O for the size exclusion fractionation.

Size exclusion fractionation

Pellets from the organic extraction were resuspended in 350 μL dH_2O. 150 μL of this resuspension was set aside for the seedling growth inhibition assay. The remaining 200 μL was loaded into 0.5 mL Amicon Ultra centrifugal filter devices with a nominal molecular weight limit of either 3,000, 10,000, or 30,000. Samples were centrifuged in a Labnet Prism microcentrifuge (14,000 x g; 30 min), flow-through was collected and diluted to 150 μL in dH_2O for the seedling growth inhibition assay. Filter tubes were then inverted in the

sample collection tubes and centrifuged in a Labnet Prism microcentrifuge (14,000 x g; 15 min) to collect the sample larger than the size cutoff. Flow-through was collected and diluted to 150 μL in dH_2O for the seedling growth inhibition assay.

QUANTIFICATION AND STATISTICAL ANALYSIS

All statistical tests were performed using the JMP Pro 14 software using $p = 0.05$. Means are calculated from at least three experimental replicates. Specific statistical tests and statistical parameters are noted in the method details and Figure Legends. OMV size distributions were calculated using FIJI.

For bacterial challenge experiments, colony counts were log transformed to approximate normality. Log-transformed counts were then normalized to the buffer control to account for variation between experimental replicates. To normalize, each log-transformed count in both buffer control and treatment samples was divided by the mean of the log-transformed counts from the buffer control. This approach preserves the variation within all conditions and allows for accurate statistical comparison. Standard error was calculated from the log-transformed, normalized points and treatment conditions were compared using ANOVA followed by a Tukey HSD post hoc test with $p = 0.05$. In all plots, scatter points indicate log-transformed, normalized values for each plant used in the experiment. Horizontal lines indicate mean of the log-transformed, normalized data for each condition, and error bars indicate standard error. Figures 1C and 2C are presented as log-transformed data without normalization to provide readers with a reference for total *Pst* amount. All plots display data from at least three independent experimental replicates each with at least seven plants per condition.

For seedling growth inhibition experiments, each seedling weight was normalized to the buffer control by dividing each weight by the mean of the buffer control samples. Each buffer control seedling weight was also normalized to the buffer control mean to preserve variation within the condition. Mean and standard error are indicated by the horizontal bars and error bars, respectively, and were calculated from the normalized data points. Scatter points indicate weight values from each seedling used in the experiment. Conditions were compared using ANOVA and a Tukey HSD post hoc test with $p = 0.05$. All plots display data from at least three independent experimental replicates each with at least seven plants per condition.

For *ICS1* experiments, conditions were compared using a Repeated-measures ANOVA with time as the repeated-measure. Luminescence was measured over time in the same plants. Upon revealing a difference at $p = 0.05$, data were subdivided by time point, and differences between conditions were assessed using an ANOVA at $p = 0.05$. All plots display data from at least three independent experimental replicates each with at least seven plants per condition.